arXiv:1610.03038v2 [hep-ph] 27 Oct 2016

A closer look at the R_D and R_{D^*} anomalies

Debjyoti Bardhan [a,1], Pritibhajan Byakti [b,2], Diptimoy Ghosh [c,3]

[a] Department of Theoretical Physics, Tata Institute of Fundamental Research, 1 Homi Bhabha Road, Mumbai 400005, India.

[b] Department of Theoretical Physics, Indian Association for the Cultivation of Science, 2A & 2B, Raja S.C. Mullick Road, Jadavpur, Kolkata 700 032, India.

[c] Department of Particle Physics and Astrophysics, Weizmann Institute of Science, Rehovot 76100, Israel.

Abstract The measurement of R_D (R_{D^*}), the ratio of the branching fraction of $\overline{B} \to D\tau\bar{\nu}_\tau(\overline{B} \to D^*\tau\bar{\nu}_\tau)$ to that of $\overline{B} \to Dl\bar{\nu}_l(\overline{B} \to D^*l\bar{\nu}_l)$, shows 1.9σ (3.3σ) deviation from its Standard Model (SM) prediction. The combined deviation is at the level of 4σ according to the Heavy Flavour Averaging Group (HFAG). In this paper, we perform an effective field theory analysis (at the dimension 6 level) of these potential New Physics (NP) signals assuming $\mathrm{SU(3)_C \times SU(2)_L \times U(1)_Y}$ gauge invariance. We first show that, in general, R_D and R_{D^*} are theoretically independent observables and hence, their theoretical predictions are not correlated. We identify the operators that can explain the experimental measurements of R_D and R_{D^*} individually and also together. Motivated by the recent measurement of the τ polarisation in $\overline{B} \to D^*\tau\bar{\nu}_\tau$ decay, $P_\tau(D^*)$ by the Belle collaboration, we study the impact of a more precise measurement of $P_\tau(D^*)$ (and a measurement of $P_\tau(D)$) on the various possible NP explanations. Furthermore, we show that the measurement of R_{D^*} in bins of q^2, the square of the invariant mass of the lepton-neutrino system, along with the information on τ polarisation and the forward-backward asymmetry of the τ lepton, can completely distinguish the various operator structures. We also provide the full expressions of the double differential decay widths for the individual τ helicities in the presence of all the 10 dimension-6 operators that can contribute to these decays.

[1] debjyoti@theory.tifr.res.in [2] tppb@iacs.res.in [3] diptimoy.ghosh@weizmann.ac.il

Contents

1 Introduction **2**

2 Operator basis **5**

3 Observables **6**

4 $\bar{B} \to D$ form factors **7**

5 $\bar{B} \to D^*$ form factors **11**

6 Expressions for a_ℓ^D, b_ℓ^D and c_ℓ^D for $\overline{B} \to D\ell\bar{\nu}_\ell$ **14**

7 Expressions for $a_\ell^{D^*}$, $b_\ell^{D^*}$ and $c_\ell^{D^*}$ for $\overline{B} \to D^*\ell\bar{\nu}_\ell$ **15**

8 Results **16**
8.1 Explaining R_D alone 16
8.2 Explaining R_{D^*} alone 17
8.3 Explaining R_D and R_{D^*} together 21

9 Summary **22**

A Full expressions for a_ℓ^D, b_ℓ^D and c_ℓ^D **24**

B Full expressions for $a_\ell^{D^*}$, $b_\ell^{D^*}$ and $c_\ell^{D^*}$ **26**

C Contribution of the Tensor operator $\mathcal{O}_{\rm TL}^{cb\ell}$ **31**
C.1 $\overline{B} \to D\tau\bar{\nu}_\tau$ 31
C.2 $\overline{B} \to D^*\tau\bar{\nu}_\tau$ 32

D $\mathrm{SU(3)_C} \times \mathrm{SU(2)_L} \times \mathrm{U(1)_Y}$ gauge invariance **33**

1 Introduction

In recent years, a number of experimental measurements involving B meson decays have shown interesting deviations from their Standard Model (SM) expectations. Deviations have been seen both in the neutral current $b \to s$ decays [1,2][1] as well as the charged current $b \to c$ processes. The most statistically significant deviation, at the 4σ level [17], is seen in the combination of R_D and R_{D^*} which are defined as,

$$R_{D^{(*)}} = \frac{\mathcal{B}\left(\overline{B} \to D^{(*)}\tau\bar{\nu}_\tau\right)}{\mathcal{B}\left(\overline{B} \to D^{(*)}l\bar{\nu}_l\right)}\,, \tag{1}$$

[1]For theoretical implications, see for example [3–16] and the references therein.

where $l = e$ or μ. In Table 1, we collect all the relevant experimental results related to the $\overline{B} \to D^{(*)}\ell\nu_\ell$ decay processes.

List of Observables			
Observable	Experimental Results		SM Prediction
	Experiment	Measured value	
R_D	Belle	$0.375 \pm 0.064 \pm 0.026$ [18]	0.299 ± 0.011 [19]
	BaBar	$0.440 \pm 0.058 \pm 0.042$ [20, 21]	0.300 ± 0.008 [22]
	HFAG average	$0.397 \pm 0.040 \pm 0.028$ [17]	0.299 ± 0.003 [23]
			$\mathbf{0.300 \pm 0.011}$
R_{D^*}	Belle	$0.293 \pm 0.038 \pm 0.015$ [18]	
	Belle	$0.302 \pm 0.030 \pm 0.011$ [25]	
	BaBar	$0.332 \pm 0.024 \pm 0.018$ [20, 21]	
	LHCb	$0.336 \pm 0.027 \pm 0.030$ [26]	0.252 ± 0.003 [24]
	HFAG average	$0.316 \pm 0.016 \pm 0.010$ [17]	$\mathbf{0.254 \pm 0.004}$
	Belle	$0.276 \pm 0.034\ ^{+0.029}_{-0.026}$ [27]	
	Our average	0.310 ± 0.017	
$\mathcal{B}\left(\overline{B} \to D\tau\bar{\nu}_\tau\right)$	BaBar	$1.02 \pm 0.13 \pm 0.11$ % [20]	$\mathbf{0.633 \pm 0.014}$ %
$\mathcal{B}\left(\overline{B} \to D^*\tau\bar{\nu}_\tau\right)$	BaBar	$1.76 \pm 0.13 \pm 0.12$ % [20]	$\mathbf{1.28 \pm 0.09}$ %
$\mathcal{B}\left(\overline{B} \to Dl\bar{\nu}_l\right)$	HFAG average	$2.13 \pm 0.03 \pm 0.09$ % [17]	$\mathbf{2.11^{+0.12}_{-0.10}}$ %
$\mathcal{B}\left(\overline{B} \to D^*l\bar{\nu}_l\right)$	HFAG average	$4.93 \pm 0.01 \pm 0.11$ % [17]	$\mathbf{5.04^{+0.44}_{-0.42}}$%
$P_\tau\left(\overline{B} \to D\tau\bar{\nu}_\tau\right)$			0.325 ± 0.009 [28]
			$\mathbf{0.325 \pm 0.012}$
$P_\tau\left(\overline{B} \to D^*\tau\bar{\nu}_\tau\right)$	Belle	$-0.44 \pm 0.47\ ^{+0.20}_{-0.17}$ [27]	-0.497 ± 0.013 [27, 29]
			$\mathbf{-0.497 \pm 0.008}$
$\mathcal{A}_{FB}^D$			$\mathbf{-0.360^{+0.002}_{-0.001}}$
$\mathcal{A}_{FB}^{D^*}$			$\mathbf{0.064 \pm 0.014}$

Table 1: The relevant observables, their experimental measurements and the SM predictions are shown. While computing the branching ratios, we have used $V_{cb} = 0.04$. As HFAG has not yet included the latest Belle measurement of R_{D^*} in their global average, we have taken a naive weighted average of the latest Belle result and the average given by HFAG. However, since the recent Belle result has a large uncertainty, it does not affect the previous world average in any significant way. The values given in boldface are our results for the SM predictions. Note that, for the $\overline{B} \to D^*\ell\bar{\nu}_\ell$ SM predictions, the uncertainties correspond to 2σ uncertainties in the form factor parameters, see section 5 for more details.

Note that, we have used the notation ℓ to denote any lepton (e, μ or τ) and l to denote only the light leptons, e and μ.

The large statistical significance of the anomaly in R_D and R_{D^*} has spurred a lot of interest in this decay modes in the last few years [24, 29–63] and various possible theoretical explanations have been proposed.

The main purpose of this work is to identify observables which can help distinguish the different NP Lorentz structures that can potentially solve the R_D and R_{D^*} anomalies. We first perform an operator analysis of these potential NP signals by considering all the dimension-6 operators that are consistent with SM gauge invariance. We compute the values of the relevant Wilson coefficients (WCs) that explain the experimental measurements within their 1σ ranges. For these values of the WCs, we compute the predictions for a few observables that have the potential to distinguish between the various NP operators. Although we provide numerical results only for the operators that are consistent with SM gauge invariance, we provide the analytical expressions for the double differential decay rates for the individual τ helicities for all the 10 independent dimension-6 operators contributing to these decays. To our knowledge, we are the first in the literature to provide the full expressions.

As we show later, R_D and R_{D^*} are in general theoretically independent observables and the anomalies can exist independently. A future measurement might reveal a greater anomaly in one of them without affecting the other. Hence, in this paper, we attempt to explain each without worrying about the other initially, but then also point out how both can be explained together.

Very recently, the Belle collaboration reported the first measurement of the τ-polarisation in the decay $\overline{B} \to D^* \tau \bar{\nu}_\tau$ [27]. While the uncertainty in this measurement is rather large now, motivated by the possibility of more precise measurements in the future, we investigate how such a measurement can distinguish the various NP explanations of R_D and R_{D^*}. Furthermore, we show that measurements of R_{D^*} in bins of q^2 can provide important information about the nature of short distance physics. In fact, a combination of binwise R_{D^*} and more precise measurements (that can be done in Belle II, for example) of τ polarisation in both the $\overline{B} \to D \tau \bar{\nu}_\tau$ and $\overline{B} \to D^* \tau \bar{\nu}_\tau$ decays can completely distinguish all the different NP operators. Moreover, we show that the forward-backward asymmetry of the τ lepton (in the τ - ν_τ rest frame) also has the potential to differentiate the various NP Lorentz structures.

The paper is organised as follows: In section 2 we write down all the operators relevant for this study and define the notations for the corresponding WCs. The various observables of our interest are defined in section 3. The sections 4 and 5 discuss the form factors required for the calculation of the decay amplitudes. The analytic expressions for the double differential decay widths for the individual lepton helicities are shown in sections 6 and 7. In the following section (section 8), we present all our numerical results. Finally, we summarise our findings in section 9.

The full expressions for the double differential decay widths are shown in the appendices A and B, and the contribution of the tensor operator $\mathcal{O}_{\rm TL}$ is discussed in appendix C. In appendix D, we show how our operators are related to the dimension-6 operators of [64].

2 Operator basis

The effective Lagrangian for the $b \to c\,\ell\,\bar{\nu}$ process at the dimension 6 level is given by,

$$\mathcal{L}_{\rm eff}^{b\to c\,\ell\,\nu} = \frac{2G_F V_{cb}}{\sqrt{2}} \Big(C_9^{cb\ell}\,\mathcal{O}_9^{cb\ell} + C_9^{cb\ell\,\prime}\,\mathcal{O}_9^{cb\ell\,\prime} + C_{10}^{cb\ell}\,\mathcal{O}_{10}^{cb\ell} + C_{10}^{cb\ell\,\prime}\,\mathcal{O}_{10}^{cb\ell\,\prime} + C_s^{cb\ell}\,\mathcal{O}_s^{cb\ell} + C_s^{cb\ell}\,\mathcal{O}_s^{cb\ell\,\prime} + C_p^{cb\ell}\,\mathcal{O}_p^{cb\ell} + C_p^{cb\ell\,\prime}\,\mathcal{O}_p^{cb\ell\,\prime} + C_T^{cb\ell}\,\mathcal{O}_T^{cb\ell} + C_{T5}^{cb\ell}\,\mathcal{O}_{T5}^{cb\ell} \Big) \tag{2}$$

where $\mathcal{O}_i^{cb\ell}$ constitute a complete basis of 6-dimensional operators and $C_i^{cb\ell}$ are the corresponding Wilson coefficients defined at the renormalization scale $\mu = m_b$. In the SM, $C_9^{cb\ell} = -C_{10}^{cb\ell} = 1$ and all the other WCs vanish. The full set of operators is given by:

$$\begin{aligned}
\mathcal{O}_9^{cb\ell} &= [\bar{c}\,\gamma^\mu\,\mathrm{P}_L\,b][\bar{\ell}\,\gamma_\mu\,\nu] & \mathcal{O}_9^{cb\ell\,\prime} &= [\bar{c}\,\gamma^\mu\,\mathrm{P}_R\,b][\bar{\ell}\,\gamma_\mu\,\nu] \\
\mathcal{O}_{10}^{cb\ell} &= [\bar{c}\,\gamma^\mu\,\mathrm{P}_L\,b][\bar{\ell}\,\gamma_\mu\gamma_5\,\nu] & \mathcal{O}_{10}^{cb\ell\,\prime} &= [\bar{c}\,\gamma^\mu\,\mathrm{P}_R\,b][\bar{\ell}\,\gamma_\mu\gamma_5\,\nu] \\
\mathcal{O}_s^{cb\ell} &= [\bar{c}\,\mathrm{P}_L\,b][\bar{\ell}\,\nu] & \mathcal{O}_s^{cb\ell\,\prime} &= [\bar{c}\,\mathrm{P}_R\,b][\bar{\ell}\,\nu] \\
\mathcal{O}_p^{cb\ell} &= [\bar{c}\,\mathrm{P}_L\,b][[\bar{\ell}\,\gamma_5\,\nu] & \mathcal{O}_p^{cb\ell\,\prime} &= [\bar{c}\,\mathrm{P}_R\,b][[\bar{\ell}\,\gamma_5\,\nu] \\
\mathcal{O}_T^{cb\ell} &= [\bar{c}\,\sigma^{\mu\nu}\,b][\bar{\ell}\,\sigma_{\mu\nu}\,\nu] & \mathcal{O}_{T5}^{cb\ell} &= [\bar{c}\,\sigma^{\mu\nu}\,b][\bar{\ell}\,\sigma_{\mu\nu}\gamma_5\,\nu]
\end{aligned} \tag{3}$$

The other possible tensor structures are related to $\mathcal{O}_T^{cb\ell}$ and $\mathcal{O}_{T5}^{cb\ell}$ in the following way,

$$\epsilon_{\mu\nu\alpha\beta}[\bar{c}\,\sigma^{\mu\nu}\,b][\bar{\ell}\,\sigma^{\alpha\beta}\,\nu] = -2i\mathcal{O}_{T5}^{cb\ell} \tag{4}$$

$$[\bar{c}\,\sigma^{\mu\nu}\gamma_5\,b][\bar{\ell}\,\sigma_{\mu\nu}\gamma_5\,\nu] = \mathcal{O}_T^{cb\ell} \tag{5}$$

$$[\bar{c}\,\sigma^{\mu\nu}\gamma_5\,b][\bar{\ell}\,\sigma_{\mu\nu}\,\nu] = \mathcal{O}_{T5}^{cb\ell}\,. \tag{6}$$

Note that the above basis of operators is different from the one used in some earlier literature [31, 36]. For example, the reference [31] uses the following set of operators,

$$\begin{aligned}
\mathcal{O}_{\rm VL}^{cb\ell} &= [\bar{c}\,\gamma^\mu\,b][\bar{\ell}\,\gamma_\mu\,P_L\,\nu] & \mathcal{O}_{\rm VR}^{cb\ell} &= [\bar{c}\,\gamma^\mu\,b][\bar{\ell}\,\gamma_\mu\,P_R\,\nu] \\
\mathcal{O}_{\rm AL}^{cb\ell} &= [\bar{c}\,\gamma^\mu\,\gamma_5\,b][\bar{\ell}\,\gamma_\mu\,P_L\,\nu] & \mathcal{O}_{\rm AR}^{cb\ell} &= [\bar{c}\,\gamma^\mu\,\gamma_5\,b][\bar{\ell}\,\gamma_\mu\,P_R\,\nu] \\
\mathcal{O}_{\rm SL}^{cb\ell} &= [\bar{c}\,b][\bar{\ell}\,P_L\,\nu] & \mathcal{O}_{\rm SR}^{cb\ell} &= [\bar{c}\,b][\bar{\ell}\,P_R\,\nu] \\
\mathcal{O}_{\rm PL}^{cb\ell} &= [\bar{c}\,\gamma_5\,b][[\bar{\ell}\,P_L\,\nu] & \mathcal{O}_{\rm PR}^{cb\ell} &= [\bar{c}\,\gamma_5\,b][[\bar{\ell}\,P_R\,\nu] \\
\mathcal{O}_{\rm TL}^{cb\ell} &= [\bar{c}\,\sigma^{\mu\nu}\,b][\bar{\ell}\,\sigma_{\mu\nu}\,P_L\,\nu] & \mathcal{O}_{\rm TR}^{cb\ell} &= [\bar{c}\,\sigma^{\mu\nu}\,b][\bar{\ell}\,\sigma_{\mu\nu}\,P_R\,\nu]
\end{aligned} \tag{7}$$

The Wilson coefficients of these two basis of operators are related through the following equations,

$$\begin{aligned}
C_{\rm VL}^{cb\ell} &= \frac{1}{2}\left(C_9^{cb\ell} - C_{10}^{cb\ell} + C_9^{cb\ell\,\prime} - C_{10}^{cb\ell\,\prime}\right) & C_{\rm SR}^{cb\ell} &= \frac{1}{2}\left(C_s^{cb\ell} + C_p^{cb\ell} + C_s^{cb\ell\,\prime} + C_p^{cb\ell\,\prime}\right) \\
C_{\rm AL}^{cb\ell} &= \frac{1}{2}\left(-C_9^{cb\ell} + C_{10}^{cb\ell} + C_9^{cb\ell\,\prime} - C_{10}^{cb\ell\,\prime}\right) & C_{\rm PR}^{cb\ell} &= \frac{1}{2}\left(-C_s^{cb\ell} - C_p^{cb\ell} + C_s^{cb\ell\,\prime} + C_p^{cb\ell\,\prime}\right)
\end{aligned} \tag{8}$$

$$
\begin{aligned}
C_{\rm SL}^{cb\ell} &= \frac{1}{2}\left(C_s^{cb\ell} - C_p^{cb\ell} + C_s^{cb\ell\,\prime} - C_p^{cb\ell\,\prime}\right) & C_{\rm VR}^{cb\ell} &= \frac{1}{2}\left(C_9^{cb\ell} + C_{10}^{cb\ell} + C_9^{cb\ell\,\prime} + C_{10}^{cb\ell\,\prime}\right) \\
C_{\rm PL}^{cb\ell} &= \frac{1}{2}\left(-C_s^{cb\ell} + C_p^{cb\ell} + C_s^{cb\ell\,\prime} - C_p^{cb\ell\,\prime}\right) & C_{\rm AR}^{cb\ell} &= \frac{1}{2}\left(-C_9^{cb\ell} - C_{10}^{cb\ell} + C_9^{cb\ell\,\prime} + C_{10}^{cb\ell\,\prime}\right) \\
C_{\rm TL}^{cb\ell} &= \left(C_T^{cb\ell} - C_{T5}^{cb\ell}\right) & C_{\rm TR}^{cb\ell} &= \left(C_T^{cb\ell} + C_{T5}^{cb\ell}\right)
\end{aligned} \tag{9}
$$

We now assume the neutrino in the final state to be left handed. This implies that the WCs in eq. (2) satisfy the following relations,

$$
\begin{aligned}
C_9^{cb\ell} &= -C_{10}^{cb\ell} && (10)\\
C_9^{cb\ell\,\prime} &= -C_{10}^{cb\ell\,\prime} && (11)\\
C_s^{cb\ell} &= -C_p^{cb\ell} && (12)\\
C_s^{cb\ell\,\prime} &= -C_p^{cb\ell\,\prime} && (13)\\
C_T^{cb\ell} &= -C_{T5}^{cb\ell}\,. && (14)
\end{aligned}
$$

Consequently, all the WCs in the right hand column of eq. 9 vanish. Note that, the operators on the left hand column of eq. 9 are the only ones that are consistent with the full gauge invariance of the SM. In appendix D, we show how these WCs are related to the 6-dimensional operators listed in [64]. Moreover, since many microscopic models do not generate the tensor operator, we neglect them in the main text and study its effect only in the appendix (see appendix C).

Although, we do not study the effects of the operators with a right handed neutrino (the ones in the right hand column of eq. 9), we compute the full analytic expressions considering all the 10 operators for the first time in the literature. The results are presented in appendices A and B.

3 Observables

The double differential branching fractions for the decays $\overline{B} \to D\ell\bar{\nu}_\ell$ and $\overline{B} \to D^*\ell\bar{\nu}_\ell$ can be written as

$$
\frac{d^2\mathcal{B}_\ell^{D^{(*)}}}{dq^2\, d(\cos\theta)} = \mathcal{N}\,|p_{D^{(*)}}|\,\left(a_\ell^{D^{(*)}} + b_\ell^{D^{(*)}}\cos\theta + c_\ell^{D^{(*)}}\cos^2\theta\right)\,. \tag{15}
$$

The normalisation factor, $\mathcal{N}$ and the absolute value of the $D^{(*)}$-meson momentum, $|p_{D^{(*)}}|$ are given by,

$$
\mathcal{N} = \frac{\tau_B\, G_F^2 |V_{cb}|^2 q^2}{256\pi^3 M_B^2}\left(1 - \frac{m_\ell^2}{q^2}\right)^2 \tag{16}
$$

$$
|p_{D^{(*)}}| = \frac{\sqrt{\lambda(M_B^2, M_{D^{(*)}}^2, q^2)}}{2M_B}, \tag{17}
$$

where $\lambda(a,b,c) = a^2+b^2+c^2-2(ab+bc+ca)$. The angle θ is defined as the angle between the lepton and $D^{(*)}$-meson in the lepton-neutrino centre-of-mass frame, and q^2 is the invariant mass squared of the lepton-neutrino system.

The total branching fraction is given by,

$$\mathcal{B}_\ell^{D^{(*)}} = \int \mathcal{N}\,|p_{D^{(*)}}| \left(2a_\ell^{D^{(*)}} + \frac{2}{3}c_\ell^{D^{(*)}}\right) dq^2 \tag{18}$$

The observables R_D and R_{D^*} have already been defined in eq. (1). We now define binned $R_{D^{(*)}}$ in the following way,

$$R_{D^{(*)}}[q^2\,\text{bin}] = \frac{\mathcal{B}_\tau^{D^{(*)}}[q^2\,\text{bin}]}{\mathcal{B}_l^{D^{(*)}}[q^2\,\text{bin}]} \tag{19}$$

For the decays with τ lepton in the final state, the polarisation of the τ also constitutes an useful observable and can potentially be used to distinguish the NP Lorentz structures. The τ polarisation fraction is defined in the following way,

$$P_\tau(D^{(*)}) = \frac{\Gamma_\tau^{D^{(*)}}(+) \;-\; \Gamma_\tau^{D^{(*)}}(-)}{\Gamma_\tau^{D^{(*)}}(+) \;+\; \Gamma_\tau^{D^{(*)}}(-)} \tag{20}$$

where, $\Gamma_\tau^{D^{(*)}}(+)$ and $\Gamma_\tau^{D^{(*)}}(-)$ are the decay widths for positive and negative helicity τ leptons respectively.

The τ forward-backward asymmetry, $\mathcal{A}_{FB}^{D^{(*)}}$ is defined as

$$\begin{aligned}\mathcal{A}_{FB}^{D^{(*)}} &= \frac{\int_0^{\pi/2} \frac{d\Gamma^{D^{(*)}}}{d\theta}d\theta - \int_{\pi/2}^{\pi} \frac{d\Gamma^{D^{(*)}}}{d\theta}d\theta}{\int_0^{\pi/2} \frac{d\Gamma^{D^{(*)}}}{d\theta}d\theta + \int_{\pi/2}^{\pi} \frac{d\Gamma^{D^{(*)}}}{d\theta}d\theta} \\ &= \frac{\int b_\tau^{D^{(*)}}(q^2)dq^2}{\Gamma^{D^{(*)}}}\end{aligned} \tag{21}$$

where $\Gamma^{D^{(*)}}$ is the total decay width of $D^{(*)}$ and the angle θ has already been defined above. Note that, while the branching fractions depend on the functions $a_\ell^{D^{(*)}}$ and $c_\ell^{D^{(*)}}$, the forward-backward asymmetry depends only on $b_\ell^{D^{(*)}}$. Hence, they provide complementary information on the nature of the short distance physics.

4 $\bar{B} \to D$ form factors

The hadronic matrix elements for $\bar{B} \to D$ transition are parametrised by[2]

[2]We use the convention $\epsilon^{0123} = 1$. This implies $\epsilon_{0123} = -1$.

$$\begin{aligned}
\langle D(p_D,M_D)|\bar{c}\gamma^\mu b|\bar{B}(p_B,M_B)\rangle &= F_+(q^2)\Big[(p_B+p_D)^\mu - \frac{M_B^2-M_D^2}{q^2}q^\mu\Big] \\
&\quad + F_0(q^2)\frac{M_B^2-M_D^2}{q^2}q^\mu \qquad (22)\\
\langle D(p_D,M_D)|\bar{c}\gamma^\mu\gamma_5 b|\bar{B}(p_B,M_B)\rangle &= 0 \qquad (23)\\
\langle D(p_D,M_D)|\bar{c}b|\bar{B}(p_B,M_B)\rangle &= F_0(q^2)\frac{M_B^2-M_D^2}{m_b-m_c} \qquad (24)\\
\langle D(p_D,M_D)|\bar{c}\gamma_5 b|\bar{B}(p_B,M_B)\rangle &= 0 \qquad (25)\\
\langle D(p_D,M_D)|\bar{c}\sigma^{\mu\nu} b|\bar{B}(p_B,M_B)\rangle &= -i(p_B^\mu p_D^\nu - p_B^\nu p_D^\mu)\frac{2F_T(q^2)}{M_B+M_D} \qquad (26)\\
\langle D(p_D,M_D)|\bar{c}\sigma^{\mu\nu}\gamma_5 b|\bar{B}(p_B,M_B)\rangle &= \varepsilon^{\mu\nu\rho\sigma}p_{B\rho}p_{D\sigma}\frac{2F_T(q^2)}{M_B+M_D} \qquad (27)
\end{aligned}$$

Note that Eq. (24) and Eq. (27) are not independent equations and follow from Eq. (22) and Eq. (26) respectively. Multiplying the left hand side of Eq. (22) by q_μ one gets

$$\begin{aligned}
q_\mu\langle D(p_D,m_D)|\bar{c}\gamma^\mu b|\bar{B}(p_B,M_B)\rangle &= \text{Inverse Fourier transform of } \langle D|i\partial_\mu(\bar{c}\gamma^\mu b)|B\rangle \\
&= \text{Inverse Fourier transform of } \langle D|(i\partial_\mu\bar{c}\gamma^\mu b + \bar{c}\gamma^\mu i\partial_\mu b)|B\rangle \\
&= (m_b-m_c)\langle D(p_D,M_D)|\bar{c}b|\bar{B}(p_B,M_B)\rangle \qquad (28)
\end{aligned}$$

Similarly, the term proportional to F_+ in the right hand side of Eq. (22) vanishes upon multiplication by q_μ and gives

$$\text{RHS} = F_0(q^2)(M_B^2 - M_D^2). \qquad (29)$$

Thus, Eq. (28) and Eq. (29) taken together give us Eq. (24).

In order to get Eq. (27) from Eq. (26) one has to use the identity,

$$\sigma^{\mu\nu}\gamma_5 = \frac{i}{2}\varepsilon^{\mu\nu\alpha\beta}\sigma_{\alpha\beta}\,. \qquad (30)$$

Substituting the above identity into the left hand side of Eq. (27) one gets,

$$\begin{aligned}
\langle D(p_D,M_D)|\bar{c}\sigma^{\mu\nu}\gamma_5 b|\bar{B}(p_B,M_B)\rangle &= \frac{i}{2}\varepsilon^{\mu\nu\alpha\beta}\langle D(p_D,M_D)|\bar{c}\sigma_{\alpha\beta} b|\bar{B}(p_B,M_B)\rangle \qquad (31)\\
&= \frac{i}{2}\varepsilon^{\mu\nu\alpha\beta}\left(-i(p_{B\alpha}p_{D\beta} - p_{B\beta}p_{D\alpha})\frac{2F_T(q^2)}{M_B+M_D}\right) \qquad (32)\\
&= \varepsilon^{\mu\nu\alpha\beta}p_{B\alpha}p_{D\beta}\frac{2F_T(q^2)}{M_B+M_D} \qquad (33)
\end{aligned}$$

The form factors $F_0(q^2)$ and $F_+(q^2)$ have been calculated using lattice QCD techniques

in [19][3]. They are given by the following expressions,

$$F_+(z) = \frac{1}{\phi_+(z)} \sum_{k=0}^{3} a_k^+ \, z^k \,, \tag{34}$$

$$F_0(z) = \frac{1}{\phi_0(z)} \sum_{k=0}^{3} a_k^0 \, z^k \,, \tag{35}$$

where

$$z \equiv z(q^2) = \frac{\sqrt{(M_B + M_D)^2 - q^2} - \sqrt{4 M_B M_D}}{\sqrt{(M_B + M_D)^2 - q^2} + \sqrt{4 M_B M_D}} \,.$$

The functions $\phi_+(z)$ and $\phi_0(z)$ are given by,

$$\phi_+(z) = 1.1213 \frac{(1+z)^2 (1-z)^{1/2}}{\left[(1+r)(1-z) + 2\sqrt{r}(1+z)\right]^5} \,, \tag{36}$$

$$\phi_0(z) = 0.5299 \frac{(1+z)(1-z)^{3/2}}{\left[(1+r)(1-z) + 2\sqrt{r}(1+z)\right]^4} \,, \tag{37}$$

where, $r = M_D/M_B$.

The central values, uncertainties, and correlation matrix for the parameters a_k^0 and a_k^+ are shown in tables 2 and 3.

	a_0^+	a_1^+	a_2^+	a_3^+	a_0^0	a_1^0	a_2^0	a_3^0
Values	0.01261	-0.0963	0.37	-0.05	0.01140	-0.0590	0.19	-0.03
Uncertainties	0.00010	0.0033	0.11	0.90	0.00009	0.0028	0.10	0.87

Table 2: The central values and uncertainties for the parameters a_k^0 and a_k^+ from ref. [19] (table XI of their arXiv version 1).

As the tensor form factor F_T has not been computed from lattice QCD, we have taken them from [65]. Following [65], we write $F_T(q^2)$ as,

$$F_T(q^2) = \frac{0.69}{\left(1 - \frac{q^2}{(6.4\text{GeV})^2}\right)\left(1 - 0.56 \frac{q^2}{(6.4\text{GeV})^2}\right)} \,. \tag{38}$$

In fig. 1, we show the q^2 dependences of F_0, F_+ and F_T following the above expressions.

[3]There has been another Lattice calculation of these form factors with similar results [22].

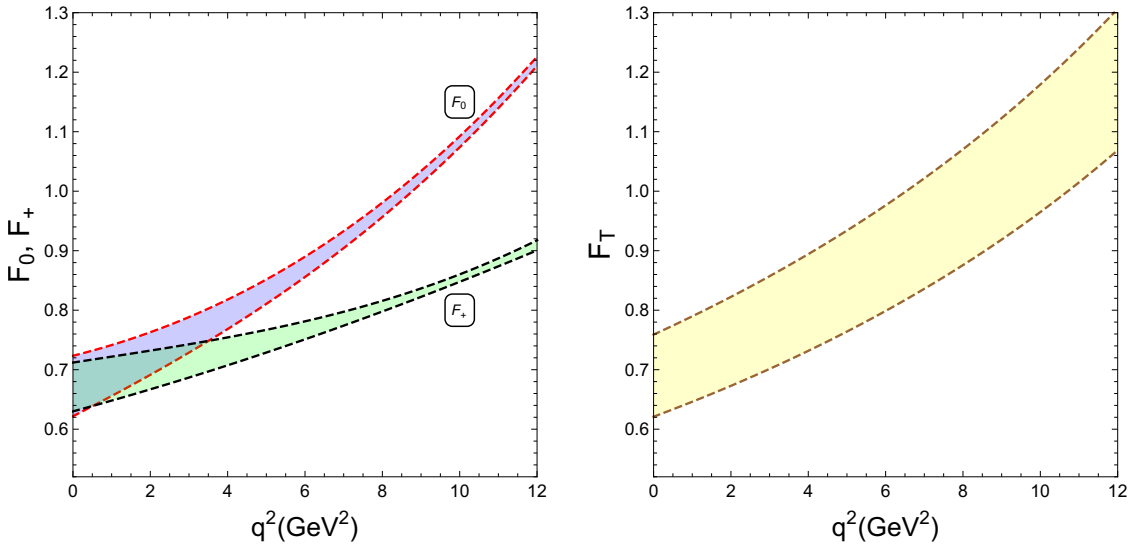

Figure 1: The q^2 dependence of the form factors F_0, F_+ and F_T. The uncertainty bands for F_0 and F_+ correspond to a $\chi^2 \leq 1.646$ where the χ^2 is computed using the expression $\chi^2(\mathbf{x}) = (\mathbf{x} - \mathbf{x_0})^T \mathbf{V}^{-1} (\mathbf{x} - \mathbf{x_0})$ where $\mathbf{x} = (a_0^+, a_1^+, a_2^+, a_3^+, a_0^0, a_1^0, a_2^0, a_3^0)$ and x_0 consists of the central values given in table 2. The covariance matrix V is computed from the correlation matrix ρ_{ij} given in table 3 using the formula $V_{ij} = \sigma_i(\mathbf{x})\rho_{ij}\sigma_j(\mathbf{x})$ where $\sigma(\mathbf{x})$ is the vector of uncertainties given in tables 2. The uncertainty band for F_T is obtained by simply taking a $\pm 10\%$ uncertainty on the central value.

	a_0^+	a_1^+	a_2^+	a_3^+	a_0^0	a_1^0	a_2^0	a_3^0
a_0^+	1.00000	0.24419	−0.08658	0.01207	0.00000	0.23370	0.03838	−0.05639
a_1^+		1.00000	−0.57339	0.25749	0.00000	0.80558	−0.25493	−0.15014
a_2^+			1.00000	−0.64492	0.00000	−0.44966	0.66213	0.05120
a_3^+				1.00000	0.00000	0.11311	−0.20100	0.23714
a_0^0					1.00000	0.00000	0.00000	0.00000
a_1^0						1.00000	−0.44352	0.02485
a_2^0							1.00000	−0.46248
a_3^0								1.00000

Table 3: The correlation matrix for the parameters a_k^0 and a_k^+ from ref. [19] (table XI of their arXiv version 1).

5 $\bar{B} \to D^*$ form factors

The hadronic matrix elements for $\bar{B} \to D^*$ transition are parametrised by

$$\langle D^*(p_{D^*}, M_{D^*})|\bar{c}\gamma_\mu b|\bar{B}(p_B, M_B)\rangle = i\varepsilon_{\mu\nu\rho\sigma}\epsilon^{\nu *} p_B^\rho p_{D^*}^\sigma \frac{2V(q^2)}{M_B + M_{D^*}} \tag{39}$$

$$\begin{aligned}\langle D^*(p_{D^*}, M_{D^*})|\bar{c}\gamma_\mu\gamma_5 b|\bar{B}(p_B, M_B)\rangle &= 2M_{D^*}\frac{\epsilon^*.q}{q^2}q_\mu A_0(q^2) + (M_B + M_{D^*})\Big[\epsilon_\mu^* - \frac{\epsilon^*.q}{q^2}q_\mu\Big]A_1(q^2) \\ &\quad - \frac{\epsilon^*.q}{M_B + M_{D^*}}\Big[(p_B + p_{D^*})_\mu - \frac{M_B^2 - M_{D^*}^2}{q^2}q_\mu\Big]A_2(q^2)\end{aligned} \tag{40}$$

$$\langle D^*(p_{D^*}, M_{D^*})|\bar{c}b|\bar{B}(p_B, M_B)\rangle = 0 \tag{41}$$

$$\langle D^*(p_{D^*}, M_{D^*})|\bar{c}\gamma_5 b|\bar{B}(p_B, M_B)\rangle = -\epsilon^*.q\,\frac{2M_{D^*}}{m_b + m_c}\,A_0(q^2) \tag{42}$$

$$\begin{aligned}\langle D^*(p_{D^*}, M_{D^*})|\bar{c}\sigma_{\mu\nu} b|\bar{B}(p_B, M_B)\rangle &= -\varepsilon_{\mu\nu\alpha\beta}\Big[- \epsilon^{\alpha *}(p_{D^*} + p_B)^\beta T_1(q^2) \\ &\quad + \frac{M_B^2 - M_{D^*}^2}{q^2}\epsilon^{*\alpha}q^\beta\left(T_1(q^2) - T_2(q^2)\right) \\ &\quad + 2\frac{\epsilon^*.q}{q^2}p_B^\alpha p_{D^*}^\beta\left(T_1(q^2) - T_2(q^2) - \frac{q^2}{M_B^2 - M_{D^*}^2}T_3(q^2)\right)\Big]\end{aligned} \tag{43}$$

$$\langle D^*(p_{D^*}, M_{D^*})|\bar{c}\sigma_{\mu\nu} q^\nu b|\bar{B}(p_B, M_B)\rangle = -2\varepsilon_{\mu\nu\rho\sigma}\epsilon^{*\nu} p_B^\rho p_{D^*}^\sigma T_1(q^2) \tag{44}$$

None of the form factors $V, A_0, A_1, A_2, T_1, T_2, T_3$ has been calculated in Lattice QCD. We used the heavy quark effective theory (HQET) form factors based on [66]. These form factors

can be written in terms of the HQET form factors in the following way [36, 66],

$$
\begin{aligned}
V(q^2) =& \frac{M_B + M_{D^*}}{2\sqrt{M_B M_{D^*}}}\, h_V(w(q^2))\,, \\
A_1(q^2) =& \frac{(M_B + M_{D^*})^2 - q^2}{2\sqrt{M_B M_{D^*}}(M_B + M_{D^*})}\, h_{A_1}(w(q^2)) \\
A_2(q^2) =& \frac{M_B + M_{D^*}}{2\sqrt{M_B M_{D^*}}} \left[h_{A_3}(w(q^2)) + \frac{M_{D^*}}{M_B} h_{A_2}(w(q^2)) \right] \\
A_0(q^2) =& \frac{1}{2\sqrt{M_B M_{D^*}}} \left[\frac{(M_B + M_{D^*})^2 - q^2}{2M_{D^*}}\, h_{A_1}(w(q^2)) \right. \\
& \left. - \frac{M_B^2 - M_{D^*}^2 + q^2}{2M_B}\, h_{A_2}(w(q^2)) - \frac{M_B^2 - M_{D^*}^2 - q^2}{2M_{D^*}}\, h_{A_3}(w(q^2)) \right] \\
T_1(q^2) =& \frac{1}{2\sqrt{M_B M_{D^*}}} \left[(M_B + M_{D^*}) h_{T_1}(w(q^2)) - (M_B - M_{D^*}) h_{T_2}(w(q^2)) \right] \\
T_2(q^2) =& \frac{1}{2\sqrt{M_B M_{D^*}}} \left[\frac{(M_B + M_{D^*})^2 - q^2}{M_B + M_{D^*}}\, h_{T_1}(w(q^2)) \right. \\
& \left. - \frac{(M_B - M_{D^*})^2 - q^2}{M_B - M_{D^*}}\, h_{T_2}(w(q^2)) \right] \\
T_3(q^2) =& \frac{1}{2\sqrt{M_B M_{D^*}}} \left[(M_B - M_{D^*}) h_{T_1}(w(q^2)) - (M_B + M_{D^*}) h_{T_2}(w(q^2)) \right. \\
& \left. - 2\frac{M_B^2 - M_{D^*}^2}{M_B} h_{T_3}(w(q^2)) \right]\,,
\end{aligned}
\tag{45}
$$

where,

$$
\begin{aligned}
h_V(w) =& R_1(w) h_{A_1}(w) \\
h_{A_2}(w) =& \frac{R_2(w) - R_3(w)}{2\, r_{D^*}} h_{A_1}(w) \\
h_{A_3}(w) =& \frac{R_2(w) + R_3(w)}{2} h_{A_1}(w) \\
h_{T_1}(w) =& \frac{1}{2(1 + r_{D^*}^2 - 2 r_{D^*} w)} \left[\frac{m_b - m_c}{M_B - M_{D^*}} (1 - r_{D^*})^2 (w+1)\, h_{A_1}(w) \right. \\
& \left. - \frac{m_b + m_c}{M_B + M_{D^*}} (1 + r_{D^*})^2 (w-1)\, h_V(w) \right] \\
h_{T_2}(w) =& \frac{(1 - r_{D^*}^2)(w+1)}{2(1 + r_{D^*}^2 - 2 r_{D^*} w)} \left[\frac{m_b - m_c}{M_B - M_{D^*}}\, h_{A_1}(w) - \frac{m_b + m_c}{M_B + M_{D^*}}\, h_V(w) \right]
\end{aligned}
\tag{46}
$$

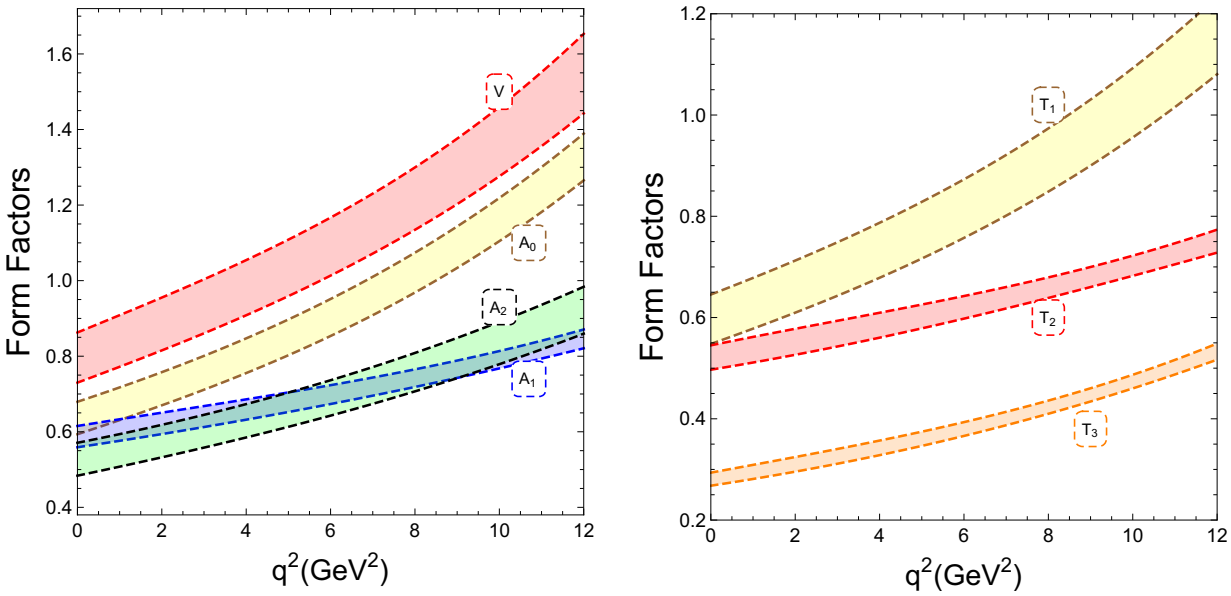

Figure 2: The q^2 dependence of the $B \to D^*$ form factors. The bands correspond to two times the uncertainties given in Eq. 49 .

$$
\begin{aligned}
h_{T_3}(w) = &- \frac{1}{2(1+r_{D^*})(1+r_{D^*}^2-2r_{D^*}w)} \left[2\frac{m_b - m_c}{M_B - M_{D^*}} r_{D^*}(w+1)\, h_{A_1}(w) \right. \\
&- \frac{m_b - m_c}{M_B - M_{D^*}}(1+r_{D^*}^2-2r_{D^*}w)(h_{A_3}(w) - r_{D^*} h_{A_2}(w)) \\
&\left. - \frac{m_b + m_c}{M_B + M_{D^*}}(1+r_{D^*})^2\, h_V(w) \right]
\end{aligned}
\tag{47}
$$

$$
\begin{aligned}
h_{A_1}(w) =& h_{A_1}(1)[1 - 8\rho_{D^*}^2 z + (53\rho_{D^*}^2 - 15)z^2 - (231\rho_{D^*}^2 - 91)z^3] \\
R_1(w) =& R_1(1) - 0.12(w-1) + 0.05(w-1)^2 \\
R_2(w) =& R_2(1) + 0.11(w-1) - 0.06(w-1)^2 \\
R_3(w) =& 1.22 - 0.052(w-1) + 0.026(w-1)^2
\end{aligned}
\tag{48}
$$

Here, $r_{D^*} = M_{D^*}/M_B$, $w(q^2) = (M_B^2 + M_{D^*}^2 - q^2)/2M_B M_{D^*}$ and $z(w) = (\sqrt{w+1} - \sqrt{2})/(\sqrt{w+1} + \sqrt{2})$.

The numerical values of the relevant parameters of the form factors along with their respective 1σ errors are given by

$$
\begin{aligned}
R_1(1) = 1.406 \pm 0.033,\ R_2(1) = 0.853 \pm 0.020,\ \rho_{D^*}^2 = 1.207 \pm 0.026\ [17] \\
h_{A_1}(1) = 0.906 \pm 0.013\ [67]\,.
\end{aligned}
\tag{49}
$$

In Fig. 2 we show the q^2 dependence of the form factors using these numerical values. As there have been no lattice calculations of these form factors, in order to be conservative, we use two times larger uncertainties than those quoted above.

6 Expressions for a_ℓ^D, b_ℓ^D and c_ℓ^D for $\overline{B} \to D\ell\bar{\nu}_\ell$

The quantities a_ℓ^D, b_ℓ^D and c_ℓ^D for positive helicity lepton are given by:

$$\begin{aligned}
a_\ell^D(+) &= \frac{2\left(M_B^2 - M_D^2\right)^2}{\left(m_b - m_c\right)^2} |\mathbf{C_{SL}^\ell}|^2 \mathbf{F_0^2} \\
&\quad + m_\ell \left[\frac{4(M_B^2 - M_D^2)^2}{q^2\left(m_b - m_c\right)} \mathcal{R}\left(\mathbf{C_{VL}^\ell C_{SL}^{\ell *}}\right) \mathbf{F_0^2}\right] \\
&\quad + m_\ell^2 \left[\frac{2\left(M_B^2 - M_D^2\right)^2}{q^4} |\mathbf{C_{VL}^\ell}|^2 \mathbf{F_0^2}\right] \qquad (50) \\
b_\ell^D(+) &= -m_\ell \left[\frac{8|p_D| M_B \left(M_B^2 - M_D^2\right)}{q^2\left(m_b - m_c\right)} \mathcal{R}\left(\mathbf{C_{SL}^\ell C_{VL}^{\ell *}}\right) \mathbf{F_0 F_+}\right] \\
&\quad - m_\ell^2 \left[\frac{8|p_D| M_B \left(M_B^2 - M_D^2\right)}{q^4} |\mathbf{C_{VL}^\ell}|^2 \mathbf{F_0 F_+}\right] \qquad (51) \\
c_\ell^D(+) &= m_\ell^2 \left[\frac{8|p_D|^2 M_B^2}{q^4} |\mathbf{C_{VL}^\ell}|^2 \mathbf{F_+^2}\right] \qquad (52)
\end{aligned}$$

Their expressions for the negative helicity lepton are,

$$\begin{aligned}
a_\ell^D(-) &= \frac{8M_B^2|p_D|^2}{q^2} |\mathbf{C_{VL}^\ell}|^2 \mathbf{F_+^2} \qquad (53) \\
b_\ell^D(-) &= 0 \qquad (54) \\
c_\ell^D(-) &= -\frac{8M_B^2|p_D|^2}{q^2} |\mathbf{C_{VL}^\ell}|^2 \mathbf{F_+^2} \qquad (55)
\end{aligned}$$

Note that, the WCs C_{AL}^ℓ and C_{PL}^ℓ do not contribute to this decay. This is because the corresponding QCD matrix elements vanish, as can be seen from eqs. (23) and (25).

The lepton mass dependence of the various terms can also be understood easily. As the vector operators do not change the chirality of the fermion line, because of the left chiral nature of the neutrino, the outgoing (negatively charged) lepton also has negative chirality (and hence negative helicity in the massless limit). Thus the production of a left-handed lepton through the vector operator does not need a mass insertion. By a similar argument, one can see that the production of a right-handed lepton through the scalar operator does not need any mass insertion. The amplitude for the production of a right-handed lepton through a vector operator, on the other hand, clearly requires a mass insertion in order to

flip the lepton helicity. This explains why the terms proportional to $|C^{\ell}_{VL}|^2$ in Eqs. 50-52 have m_ℓ^2 and the interference terms proportional to $\mathcal{R}\left(C^{\ell}_{\rm SL}C^{\ell *}_{\rm VL}\right)$ have m_ℓ in front, while there is no such dependence in Eqs. 53-55.

The full expressions for a_ℓ^D, b_ℓ^D and c_ℓ^D including all the operators in Eq. (7) are shown in appendix A.

7 Expressions for $a_\ell^{D^*}$, $b_\ell^{D^*}$ and $c_\ell^{D^*}$ for $\overline{B} \to D^* \ell \bar{\nu}_\ell$

The quantities $a_\ell^{D^*}$, $b_\ell^{D^*}$ and $c_\ell^{D^*}$ for positive and negative helicitiy leptons are given by,

$$\begin{aligned}
a_\ell^{D^*}(-) &= \frac{8M_B^2\left|p_{D^*}\right|^2}{\left(M_B+M_{D^*}\right)^2}\left|\mathbf{C^{\ell}_{VL}}\right|^2\mathbf{V^2} + \frac{\left(M_B+M_{D^*}\right)^2\left(8M_{D^*}^2q^2+\lambda\right)}{2M_{D^*}^2q^2}\left|\mathbf{C^{\ell}_{AL}}\right|^2\mathbf{A_1^2} \\
&+\frac{8M_B^4|p_{D^*}|^4}{M_{D^*}^2\left(M_B+M_{D^*}\right)^2q^2}\left|\mathbf{C^{\ell}_{AL}}\right|^2\mathbf{A_2^2} \\
&-\frac{4\left|p_{D^*}\right|^2M_B^2\left(M_B^2-M_{D^*}^2-q^2\right)}{M_{D^*}^2q^2}\left|\mathbf{C^{\ell}_{AL}}\right|^2\left(\mathbf{A_1A_2}\right) \qquad (56)
\end{aligned}$$

$$b_\ell^{D^*}(-) = -16|p_{D^*}|M_B\mathcal{R}\left(\mathbf{C^{\ell}_{VL}C^{\ell *}_{AL}}\right)\left(\mathbf{VA_1}\right) \qquad (57)$$

$$\begin{aligned}
c_\ell^{D^*}(-) &= \frac{8\left|p_{D^*}\right|^2M_B^2}{\left(M_B+M_{D^*}\right)^2}\left|\mathbf{C^{\ell}_{VL}}\right|^2\mathbf{V^2} - \frac{\left(M_B+M_{D^*}\right)^2\lambda}{2M_{D^*}^2q^2}\left|\mathbf{C^{\ell}_{AL}}\right|^2\mathbf{A_1^2} \\
&-\frac{8|p_{D^*}|^4M_B^4}{\left(M_B+M_{D^*}\right)^2M_{D^*}^2q^2}\left|\mathbf{C^{\ell}_{AL}}\right|^2\mathbf{A_2^2} \\
&+\frac{4\left|p_{D^*}\right|^2M_B^2\left(M_B^2-M_{D^*}^2-q^2\right)}{M_{D^*}^2q^2}\left|\mathbf{C^{\ell}_{AL}}\right|^2\left(\mathbf{A_1A_2}\right) \qquad (58)
\end{aligned}$$

$$\begin{aligned}
a_\ell^{D^*}(+) &= \frac{8\left|p_{D^*}\right|^2M_B^2}{\left(m_b+m_c\right)^2}\left|\mathbf{C^{\ell}_{PL}}\right|^2\mathbf{A_0^2} \\
&-m_\ell\left[\frac{16\left|p_{D^*}\right|^2M_B^2}{\left(m_b+m_c\right)q^2}\mathcal{R}\left(\mathbf{C^{\ell}_{AL}C^{\ell *}_{PL}}\right)\mathbf{A_0^2}\right] \\
&+m_\ell^2\left[\frac{8\left|p_{D^*}\right|^2M_B^2}{q^4}\left|\mathbf{C^{\ell}_{AL}}\right|^2\mathbf{A_0^2} + \frac{8\left|p_{D^*}\right|^2M_B^2}{\left(M_B+M_{D^*}\right)^2q^2}\left|\mathbf{C^{\ell}_{VL}}\right|^2\mathbf{V^2}\right. \\
&\left.+\frac{2\left(M_B+M_{D^*}\right)^2}{q^2}\left|\mathbf{C^{\ell}_{AL}}\right|^2\mathbf{A_1^2}\right] \qquad (59)
\end{aligned}$$

$$
\begin{aligned}
b_\ell^{D^*}(+) &= m_\ell \left[\frac{4|p_{D^*}| M_B \left(M_B + M_{D^*}\right) \left(M_B^2 - M_{D^*}^2 - q^2\right)}{M_{D^*} \left(m_b + m_c\right) q^2} \mathcal{R}\left(\mathbf{C_{AL}^{\ell} C_{PL}^{\ell *}}\right) \mathbf{A_0 A_1} \right. \\
&\quad \left. - \frac{16}{\left(m_b + m_c\right)} \frac{|p_{D^*}|^3 M_B^3}{\left(M_B + M_{D^*}\right) M_{D^*} q^2} \mathcal{R}\left(\mathbf{C_{AL}^{\ell} C_{PL}^{\ell *}}\right) \mathbf{A_0 A_2} \right] \\
&\quad + m_\ell^2 \left[- \frac{4|p_{D^*}| M_B \left(M_B + M_{D^*}\right)}{M_{D^*} q^4} \left(M_B^2 - M_{D^*}^2 - q^2\right) \left|\mathbf{C_{AL}^{\ell}}\right|^2 \mathbf{A_0 A_1} \right. \\
&\quad \left. + \frac{16 |p_{D^*}|^3 M_B^3}{\left(M_B + M_{D^*}\right) M_{D^*} q^4} \left|\mathbf{C_{AL}^{\ell}}\right|^2 \mathbf{A_0 A_2} \right] \qquad (60) \\
c_\ell^{D^*}(+) &= m_\ell^2 \left[- \frac{8 \left|p_{D^*}\right|^2 M_B^2}{\left(M_B + M_{D^*}\right)^2 q^2} \left|\mathbf{C_{VL}^{\ell}}\right|^2 \mathbf{V^2} + \frac{\left(M_B + M_{D^*}\right)^2 \lambda}{2 M_{D^*}^2 q^4} \left|\mathbf{C_{AL}^{\ell}}\right|^2 \mathbf{A_1^2} \right. \\
&\quad + \frac{8 |p_{D^*}|^4 M_B^4}{M_{D^*}^2 \left(M_B + M_{D^*}\right)^2 q^4} \left|\mathbf{C_{AL}^{\ell}}\right|^2 \mathbf{A_2^2} \\
&\quad \left. - \frac{4 \left|p_{D^*}\right|^2 M_B^2}{M_{D^*}^2 q^4} \left(M_B^2 - M_{D^*}^2 - q^2\right) \left|\mathbf{C_{AL}^{\ell}}\right|^2 \left(\mathbf{A_1 A_2}\right) \right] \qquad (61)
\end{aligned}
$$

The WC C_{SL}^{ℓ} does not contribute to this decay because the corresponding QCD matrix element vanishes as can be seen from eq. (41). The lepton mass dependence of the various terms can be understood in the same way as the $\overline{B} \to D\ell\bar{\nu}_\ell$ decay. Note also the absence of interference terms proportional to $\mathcal{R}\left(C_{VL}^{\ell} C_{PL}^{\ell *}\right)$ in the above expressions.

We provide the completely general result taking into account all the operators in Eq. (7) in appendix B.

8 Results

8.1 Explaining R_D alone

As mentioned in sec. 6, the $\overline{B} \to D\tau\bar{\nu}_\tau$ amplitude depends only on the WCs C_{VL}^{τ} and C_{SL}^{τ}. In Fig. 3, we show R_D as function of C_{VL}^{τ} and C_{SL}^{τ}. In the right plot, we set C_{VL}^{τ} to its SM value $C_{VL}^{\tau}|_{\rm SM} = 1$ and vary C_{SL}^{τ}, while in the left plot, we hold C_{SL}^{τ} fixed at its SM value $C_{SL}^{\tau}|_{\rm SM} = 0$ and change C_{VL}^{τ}. The red and brown shades correspond to the experimentally allowed 1σ and 2σ ranges (see Table 1), for which we have added the statistical and systematic uncertainties in quadrature.

The ranges of C_{VL}^{τ} and C_{SL}^{τ} that are consistent with R_D at 1σ are shown in the second row of Table 4. The ranges for C_{SL}^{τ} are slightly asymmetric about zero because of its interference with C_{VL}^{τ}. In the rows 3, 4 and 5-8, we also show the predictions for $P_\tau(D)$, $\mathcal{A}_{FB}^{D}$ and R_D in four different bins for the allowed ranges of C_{VL}^{τ} and C_{SL}^{τ}. Note that, $\mathcal{A}_{FB}^{D}$ and the polarisation fraction $P_\tau(D)$ are independent of C_{VL}^{τ} if C_{SL}^{τ} is set to zero. This is because, in this case the differential decay rate is proportional to $|C_{VL}^{\tau}|^2$ and hence, the dependence on C_{VL}^{τ} drops out in $P_\tau(D)$ and $\mathcal{A}_{FB}^{D}$. This is why the ranges for $P_\tau(D)$ and $\mathcal{A}_{FB}^{D}$ in the third and fourth columns are identical. The binwise R_D values are also graphically represented in

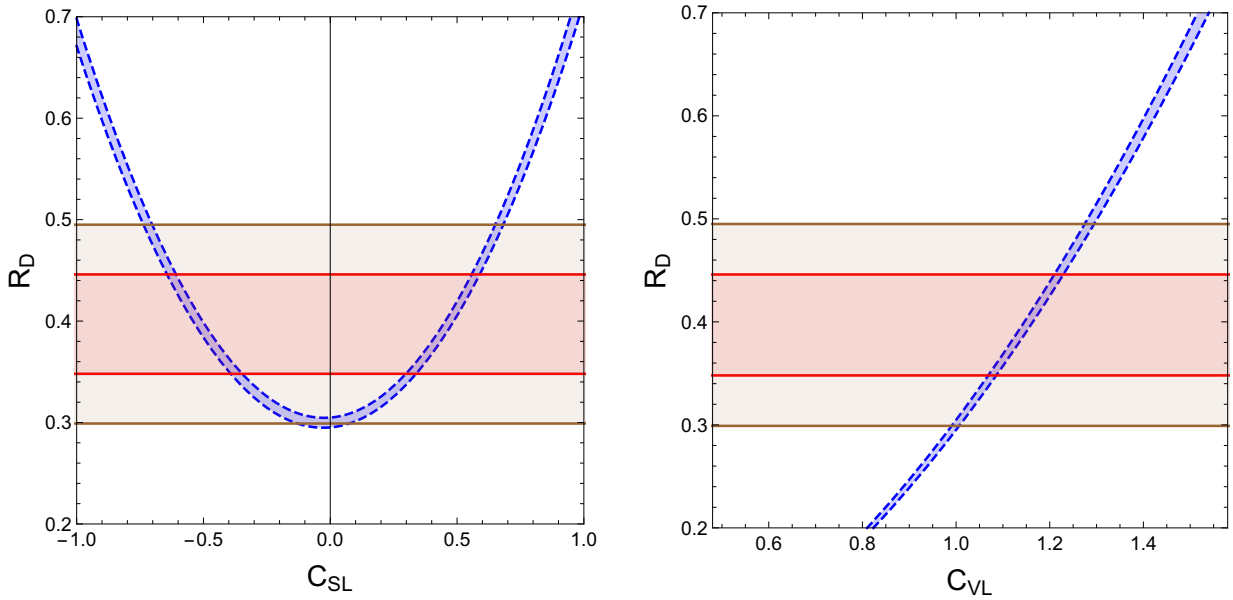

Figure 3: The dependence of R_D with respect to the variation of the WCs C_{VL}^{τ} (left) and C_{SL}^{τ} (right).

Fig. 4. The left and the right panels correspond to the WCs C_{VL}^{τ} and C_{SL}^{τ} respectively. The SM predictions are shown in red. One can conclude from Fig. 4 that the binwise R_D does not help distinguish the two WCs C_{VL}^{τ} and C_{SL}^{τ}.

The predictions for $P_\tau(D)$, $\mathcal{A}_{FB}^{D}$ are pictorially presented in the left and middle panel of Fig. 5. As mentioned earlier, in the absence of C_{SL}^{τ}, $P_\tau(D)$ and $\mathcal{A}_{FB}^{D}$ are completely independent of C_{VL}^{τ}. Hence, neither measurement can distinguish between $C_{VL}^{\tau} = 1$ and other values of C_{VL}^{τ}. However, the predictions are very different for C_{SL}^{τ}. Therefore, a measurement of $P_\tau(D)$ will tell us whether NP in the form of scalar operator $\mathcal{O}_{SL}^{cb\tau}$ exists or not. Moreover, the two separate ranges of C_{SL}^{τ} which satisfy the experimental bounds give very different values of $\mathcal{A}_{FB}^{D}$, indicated by the subscripts "+" and "-" in the middle figure.

In the right panel of Fig. 5, we also show the differential decay width as a function of q^2. As for the case of $P_\tau(D)$ and $\mathcal{A}_{FB}^{D}$, the differential decay width is independent of C_{VL}^{τ} for $C_{SL}^{\tau} = 0$. The blue solid line is the SM prediction, and the black and red dashed lines are the predictions for two representative values of C_{SL}^{τ}, $C_{SL}^{\tau} = -0.650$ and 0.310 respectively. While producing these plots, we have used the central values of the form factors. The blue data points are from the BaBar measurement reported in [21]. It is clear that the differential decay width is not a good discriminant of the various NP operators.

8.2 Explaining R_{D^*} alone

The $\overline{B} \to D^* \tau \bar{\nu}_\tau$ decay amplitude depends on three WCs, $C_{VL}^{\tau}, C_{AL}^{\tau}$ and C_{PL}^{τ}. In Fig. 6, we show R_{D^*} as function of these WCs. In each of the plots, the WCs that are not varied are all

		SM	$\mathbf{C_{VL}}$ ($\mathbf{C_{SL}} = 0$)	$\mathbf{C_{SL}}$ ($\mathbf{C_{VL}} = 1$)
	1σ range of the WC		[1.073, 1.222]	[−0.656, −0.342] [0.296, 0.596]
	$P_\tau(D)$	[0.313, 0.336]	[0.313, 0.336]	[0.408, 0.556]
	$\mathcal{A}_{FB}^D$	[−0.361, −0.358]	[−0.361, −0.358]	[−0.168, −0.022] [−0.450, −0.428]
R_D [bin]	$[m_\tau^2 - 5]$ GeV^2	[0.154, 0.158]	[0.178, 0.236]	[0.161, 0.181]
	$[5 - 7]$ GeV^2	[0.578, 0.593]	[0.665, 0.888]	[0.626, 0.752]
	$[7 - 9]$ GeV^2	[0.980, 1.003]	[1.127, 1.505]	[1.125, 1.502]
	$[9 - (M_B - M_D)^2]$ GeV^2	[1.776, 1.823]	[2.049, 2.741]	[2.294, 3.669]

Table 4: The values of the WCs consistent with the 1σ experimental range for R_D are shown in the second row. The subsequent rows show the predictions for $P_\tau(D)$, $\mathcal{A}_{FB}^D$ and R_D in four q^2 bins for the WC ranges shown in the second row.

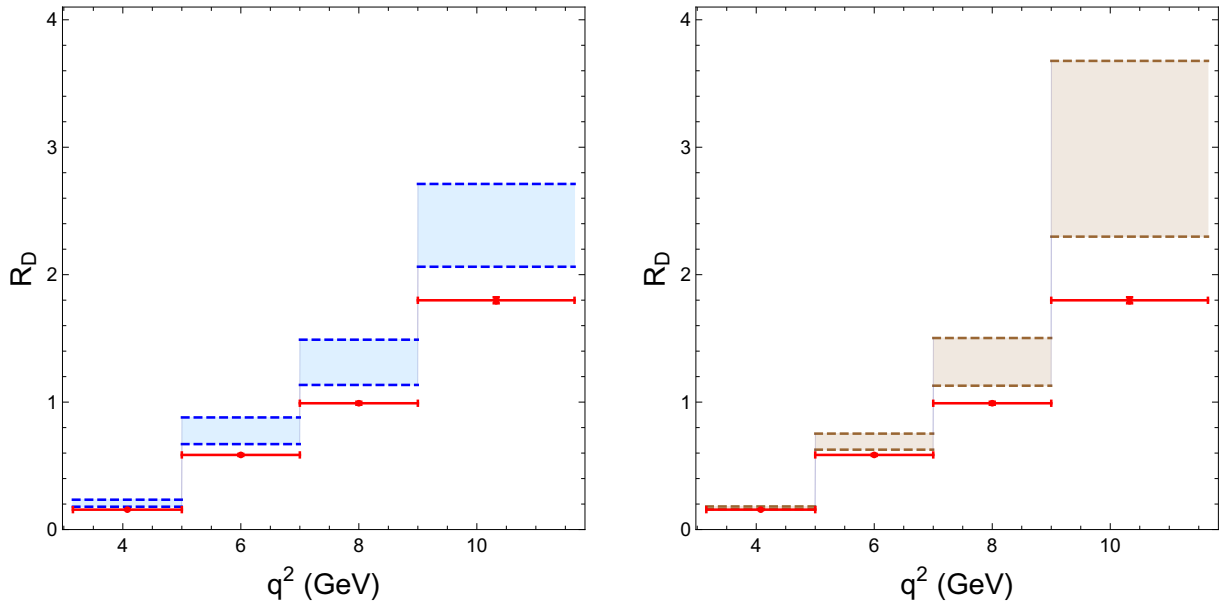

Figure 4: The binwise R_D for four q^2 bins. On the left, C_{VL}^τ is varied, while on the right, C_{SL}^τ is varied within their 1σ allowed ranges.

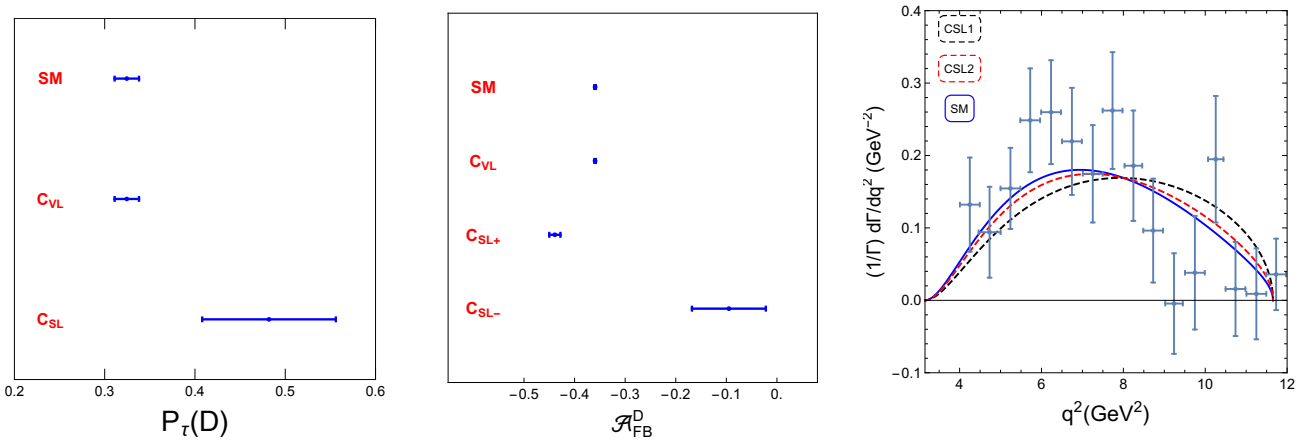

Figure 5: Predictions for the polarisation fraction $P_\tau(D)$ (left), $\mathcal{A}_{FB}^{D}$ (middle) and the differential decay width (right). The subscripts "+" and "-" in the middle figure correspond to the two ranges of C_{SL}^τ that satisfy the experimental bounds of R_D. In the right graph, the solid blue line is the SM prediction. The dashed black and red lines correspond to $C_{SL}^\tau = -0.650$ and 0.310 respectively. The data points shown on the right plot are due to the BaBar collaboration and are taken from [21].

set to their SM values. The red and brown shades correspond to the experimentally allowed 1σ and 2σ ranges respectively (see table 1).

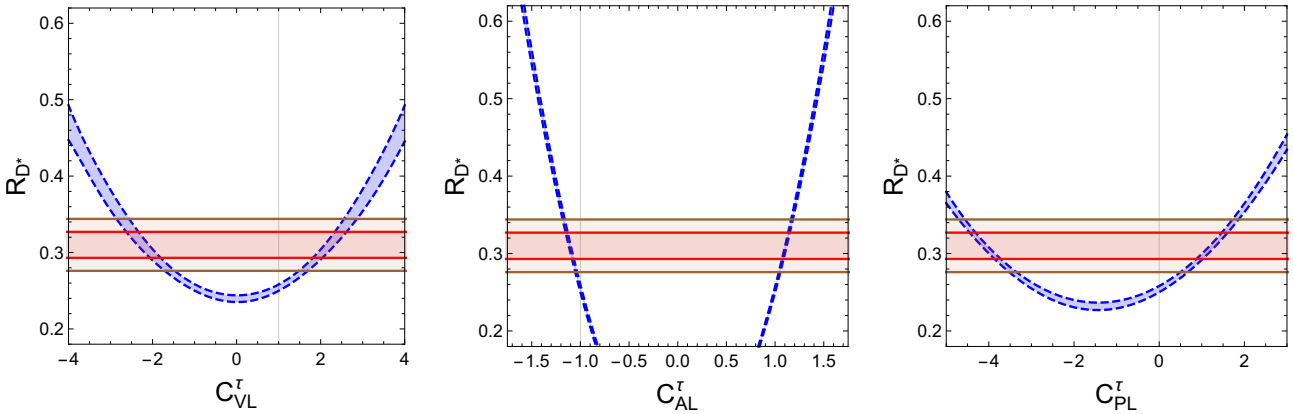

Figure 6: The dependence of R_{D^*} with respect to the variation of the WCs C_{VL}^τ (left), C_{AL}^τ (middle) and C_{PL}^τ (right). A thin vertical line shows the SM values of the WCs.

The ranges of C_{VL}^τ, C_{AL}^τ and C_{PL}^τ that are consistent with the experimental value of R_{D^*} at 1σ are shown in the second row of Table 5. We only show the ranges that are closest

to the SM values of the WCs. In the rows 3, 4 and 5-8, we also show the predictions for $P_\tau(D^*)$, $\mathcal{A}_{FB}^{D^*}$ and R_{D^*} in four different bins for these allowed ranges of C_{VL}^τ, C_{AL}^τ and C_{PL}^τ.

The binwise R_{D^*} values are also plotted in Fig. 7. The left, middle and the right panels correspond to the variation of WCs C_{VL}^τ, C_{AL}^τ and C_{SL}^τ respectively. The 1σ and 2σ experimental values are shown in red and brown respectively. It can be seen that R_{D^*} in the last bin can be used to distinguish between C_{VL}^τ(or C_{PL}^τ) and C_{AL}^τ.

		SM	$\mathbf{C_{VL}}$ $\mathbf{C_{AL,PL}} = -1, 0$	$\mathbf{C_{AL}}$ $\mathbf{C_{VL,PL}} = 1, 0$	$\mathbf{C_{PL}}$ $\mathbf{C_{VL,AL}} = 1, -1$
	Range in WC		[1.856, 2.569]	[−1.149, −1.073]	[0.890, 1.583]
	$P_\tau(D^*)$	[−0.505, −0.490]	[−0.530, −0.509]	[−0.505, −0.488]	[−0.322, −0.144]
	$\mathcal{A}_{FB}^{D^*}$	[0.050, 0.078]	[0.191, 0.297]	[0.028, 0.062]	[−0.078, −0.007]
R_{D^*} [bin]	$[m_\tau^2 - 5]$ GeV^2	[0.103, 0.105]	[0.120, 0.140]	[0.116, 0.132]	[0.124, 0.148]
	$[5 - 7]$ GeV^2	[0.331, 0.336]	[0.387, 0.457]	[0.373, 0.425]	[0.390, 0.465]
	$[7 - 9]$ GeV^2	[0.475, 0.479]	[0.535, 0.613]	[0.535, 0.613]	[0.534, 0.610]
	$[9 - (M_B - M_{D^*})^2]$ GeV^2	[0.554, 0.556]	[0.577, 0.619]	[0.621, 0.710]	[0.571, 0.611]

Table 5: The values of the WCs consistent with the 1σ experimental range for R_D^* are shown in the second row. We only show the ranges that are closest to the SM values of the WCs. The subsequent rows show the predictions for $P_\tau(D^*)$, $\mathcal{A}_{FB}^{D^*}$ and R_{D^*} in four q^2 bins for the WC ranges shown in the second row.

The predictions for $P_\tau(D^*)$ are pictorially presented in the left panel of Fig. 8. We do not show the recent Belle measurements in this figure because the uncertainties are rather large. Instead, we show a projection for Belle II 20 ab^{-1} (which is expected to be collected by the end of 2021 [68]) assuming that the systematic uncertainty will go down by a factor of two compared to that in the recent Belle measurement. It can be seen that Belle II with 20 ab^{-1} data will be able to distinguish C_{PL}^τ with the other WCs. The middle panel of Fig. 8 shows the predictions of $\mathcal{A}_{FB}^{D^*}$ pictorially. It can be seen that a measurement of $\mathcal{A}_{FB}^{D^*}$ can also potentially differentiate the various operators. In the right panel of Fig. 8, we show the normalised differential decay width as a function of q^2 for some representative values of the WCs from Table 5. It can be seen that the shape of the distribution does not change dramatically across the various NP explanations of R_{D^*}.

In Fig. 9, we show the predictions for $P_\tau(D^*)$, R_{D^*} in the last bin and $\mathcal{A}_{FB}^{D^*}$ in three different planes for the three WCs C_{VL}^τ, C_{AL}^τ and C_{PL}^τ when their values are restricted to the ranges shown in Table 5. Interestingly, we find that each of the three pairs of observables can potentially distinguish between the WCs unambiguously. Hence, the measurements of these observables by the experimental collaborations ought to be very much on the cards in their future runs.

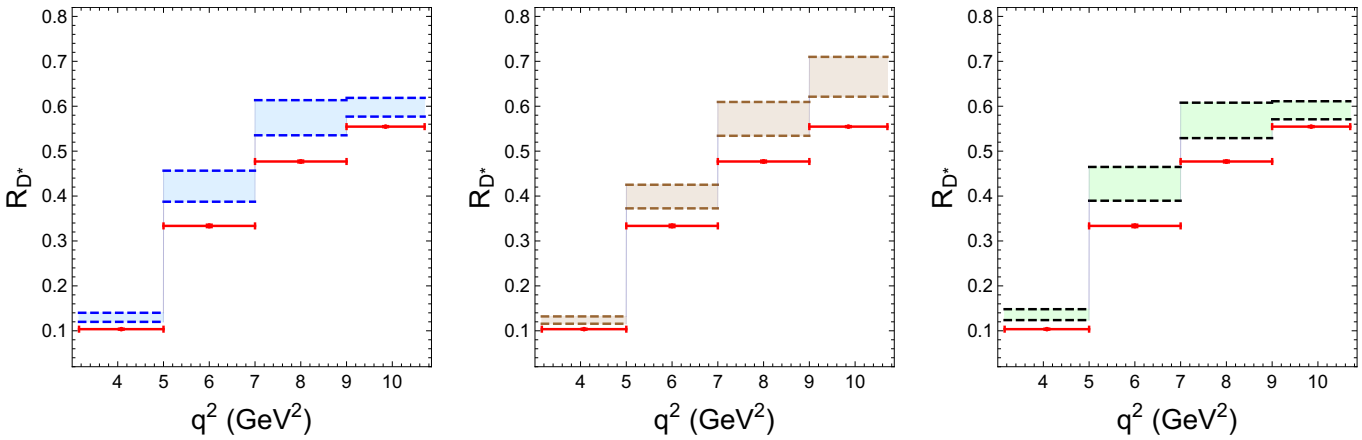

Figure 7: The binwise R_D^* for four q^2 bins. On the left, C_{VL}^τ is varied, in the middle C_{AL}^τ is varied, annd on the right, C_{PL}^τ is varied within their 1σ allowed ranges. The SM predictions are shown in red.

8.3 Explaining R_D and R_{D^*} together

We have seen from section 8.1 and 8.2 that while R_D gets contributions from C_{VL}^τ and C_{SL}^τ, R_{D^*} is affected by C_{VL}^τ, C_{AL}^τ and C_{PL}^τ. Therefore, in general, these two observables are theoretically independent. In the basis of WCs defined by $\{C_{VL}^\tau, C_{AL}^\tau, C_{SL}^\tau, C_{PL}^\tau\}$, the C_{VL}^τ direction is the only direction that affects both. However, as can be seen from tables 4 and 5, the range of C_{VL}^τ (i.e., [1.073, 1.222]) that explains R_D within 1σ is different from the range (i.e., [1.849, 2.648]) that explains R_{D^*} successfully within 1σ. Thus R_D and R_{D^*} can not be explained simultaneously by invoking NP only of type C_{VL}^τ. Fig. 10 shows the allowed region in the $C_{VL}^\tau - C_{AL}^\tau$ plane by the R_D and R_{D^*} measurements. As C_{AL}^τ does not contribute to the $\overline{B} \to D\tau\bar{\nu}_\tau$ decay, the allowed region for C_{VL}^τ from R_D (the red region) is independent of the value of C_{AL}^τ. On the other hand, both the WCs C_{VL}^τ and C_{AL}^τ contribute to the $\overline{B} \to D^*\tau\bar{\nu}_\tau$ decay and hence the values of these WCs allowed by R_{D^*} measurement are correlated. The overlap of the red and the green regions correspond to $C_{VL}^\tau \in [1.073, 1.222]$ and $C_{AL}^\tau \in [-1.144, -1.062]$.

Hence, a minimum value of $C_{VL}^\tau \approx -C_{AL}^\tau \approx 1.07$ which translates to $\Delta(C_9 - C_{10}) \approx 0.15$ (i.e, 15% shift from the SM values) can explain both R_D and R_D^* successfully. This correspond to the operator $[\bar{c}\,\gamma^\mu\,\mathrm{P}_L\,b][\bar{\ell}\,\gamma_\mu \mathrm{P}_L\,\nu]$ with a coefficient g_{NP}^2/Λ^2 where Λ is given by $\Lambda \approx g_{\rm NP}\ 2.25$ TeV.

The predictions for $P_\tau(D^*)$, $\mathcal{A}_{FB}^{D^*}$ and binwise R_{D^*} for the above ranges of C_{VL}^τ and C_{AL}^τ are given in table 6.

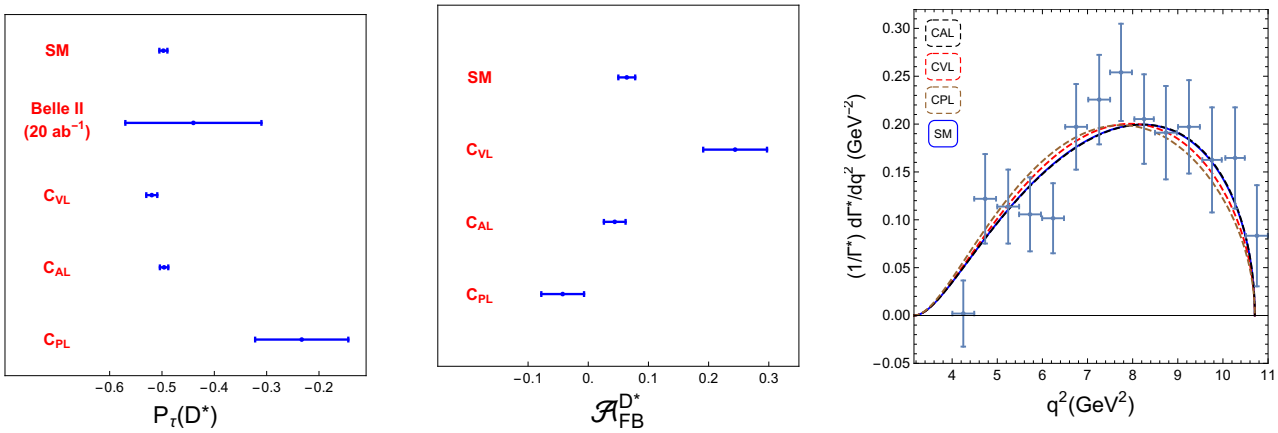

Figure 8: Predictions for the polarisation fraction $P_\tau(D^*)$ (left), $\mathcal{A}_{FB}^{D^*}$ (middle) and the differential decay width (right). In the left plot, the Belle II 20 ab^{-1} projection is obtained by i) scaling down the statistical uncertainty of the recent Belle measurement by the ratio of the luminosities i.e., $\sqrt{20/0.71}$ ii) assuming the systematic uncertainty to go down by a factor of two, and adding them in quadrature. The central value is assumed to remain unchanged. On the right plot, The solid blue line is the SM prediction. The dashed black, red and brown lines correspond to $C_{AL}^\tau = -1.12$, $C_{VL}^\tau = 1.9$ and $C_{PL}^\tau = 1.5$ respectively, where in each case every other WC is set to their SM values. Note that the black dotted curve is indistinguishable from the SM curve. The data is due to a BaBar measurement reported in [21].

C_{VL}^τ	$P_\tau(D^*)$	R_{D^*} [bin]			
$\in$ [1.073, 1.222]	$\in$ [-0.507, -0.489]	$[m_\tau^2 - 5]$ GeV^2	[5 − 7] GeV^2	[7 − 9] GeV^2	$[9 - (M_B - M_{D^*})^2]$ GeV^2
C_{AL}^τ $\in$ [-1.144, -1.067]	$\mathcal{A}_{FB}^{D^*}$ $\in$ [0.055, 0.092]	[0.116, 0.131]	[0.373, 0.426]	[0.535, 0.609]	[0.616, 0.706]

Table 6: Predictions for $P_\tau(D^*)$, $\mathcal{A}_{FB}^{D^*}$ and binwise R_{D^*} for the values of WCs satisfying both the observations simultaneously. The 1σ range of the WCs is given in the first column.

9 Summary

In this paper we have performed a model independent analysis of the R_D and R_{D^*} anomalies using dimension-6 operators that arise in a gauge invariant way. Among the four WCs C_{VL}^τ, C_{AL}^τ, C_{SL}^τ and C_{PL}^τ, only C_{VL}^τ and C_{SL}^τ contribute to R_D. On the other hand, R_{D^*} gets contributions from C_{VL}^τ, C_{AL}^τ and C_{PL}^τ. Thus, C_{VL}^τ is the only WC that affects both (barring tensor operator that is discussed in appendix C) and hence, these two observables are in general theoretically independent. In view of this, initially we studied the solutions of R_D and R_{D^*} anomalies independent of each other. We obtained the ranges of the WCs that

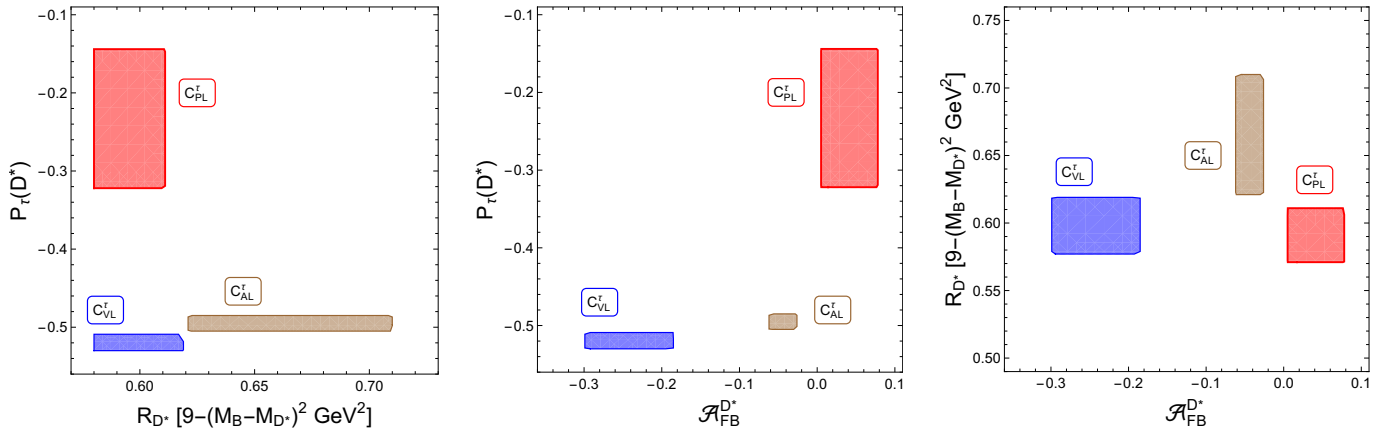

Figure 9: The predictions for $P_\tau(D^*)$, R_{D^*} in the last bin and $\mathcal{A}_{FB}^{D^*}$ are shown in three different planes for the ranges of the three WCs C_{VL}^τ, C_{AL}^τ and C_{PL}^τ given in Table 5. We remind the readers that, we have inflated the uncertainties in the form factor parameters in Eq. (49) by a factor of two. Hence, the ranges of $P_\tau(D^*)$ and R_{D^*} shown here are rather conservative.

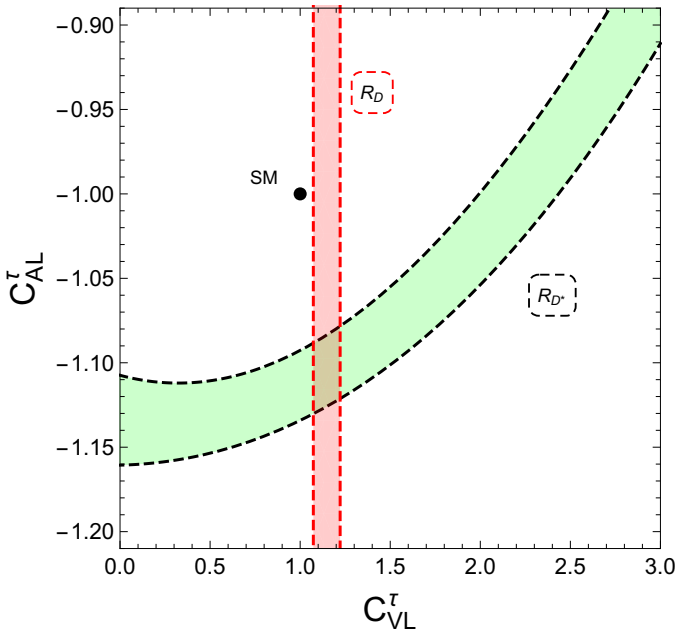

Figure 10: Allowed region in the $C_{VL}^\tau - C_{AL}^\tau$ plane by R_D and R_{D^*} measurements .

are allowed by the R_D and R_D^* measurements at 1σ. We also discussed the possibility of simultaneous solutions of these two anomalies.

For the allowed ranges of the WCs, we computed the predictions for both R_D and R_{D^*} in four different q^2 bins, the forward-backward asymmetry, $\mathcal{A}_{FB}^{D^{(*)}}$ and the polarisation fraction of the final state τ lepton. We show that measuring the τ polarisation in $\overline{B} \to D^* \tau \bar{\nu}_\tau$ decays along with the value of R_{D^*} in the last q^2 bin can distinguish between the three WCs which contribute to this process. This is graphically presented in Fig. 9. Similarly, as seen in Fig. 5, the measurement of the τ polarisation in $\overline{B} \to D \tau \bar{\nu}_\tau$ decay can in principle be used to distinguish the two WCs C_{VL}^τ and C_{SL}^τ. Furthermore, we find that the forward-backward asymmetry of the τ lepton is also a powerful discriminant of the various WCs (see Figs. 5 and 9). Unlike $P_\tau(D)$, it can even distinguish the sign of the scalar operator for the $\overline{B} \to D \tau \bar{\nu}_\tau$ decay. We hope that the experimental collaborations will take a note of this and make these measurements in near future.

Additionally, in the appendix we also provide the analytic expressions for the double differential decay widths for individual τ helicities taking into account all the 10 dimension-6 operators listed out in section 2. To our knowledge, we are the first to provide the full expressions in the literature.

Although we have not considered the tensor operator $\mathcal{O}_{\rm TL}$ in the main text, we have explored its effects on the R_D and R_D^* anomalies in appendix C. We have shown that there exists a small range of $C_{\rm TL}$ that is consistent with both the anomalies.

Acknowledgement

We thank Abhishek M. Iyer for collaboration in the very first stage of this work.

Appendix

A Full expressions for a_ℓ^D, b_ℓ^D and c_ℓ^D

For the negative helicity of the lepton:

$$\begin{aligned}
\frac{1}{8} a_\ell^D(-) &= \frac{M_B^2 |p_D|^2}{q^2} \boxed{|\mathbf{C_{VL}^\ell}|^\mathbf{2} \mathbf{F_+^2}} + \frac{\left(M_B^2 - M_D^2\right)^2}{4\left(m_b - m_c\right)^2} |\mathbf{C_{SR}^\ell}|^\mathbf{2} \mathbf{F_0^2} \\
&+ m_\ell \left[\frac{\left(M_B^2 - M_D^2\right)^2}{2q^2 (m_b - m_c)} \mathcal{R}\left(\mathbf{C_{SR}^\ell C_{VR}^{\ell *}}\right) \mathbf{F_0^2} + \frac{4 M_B^2 |p_D|^2}{q^2 \left(M_B + M_D\right)} \mathcal{R}\left(\mathbf{C_{TL}^\ell C_{VL}^{\ell *}}\right) \mathbf{F_+ F_T} \right] \\
&+ m_\ell^2 \left[\frac{\left(M_B^2 - M_D^2\right)^2}{4q^4} |\mathbf{C_{VR}^\ell}|^\mathbf{2} \mathbf{F_0^2} + \frac{4 |p_D|^2 M_B^2}{q^2 \left(M_B + M_D\right)^2} |\mathbf{C_{TL}^\ell}|^\mathbf{2} \mathbf{F_T^2} \right] \qquad (62)
\end{aligned}$$

$$
\begin{aligned}
\frac{1}{8}b_\ell^D(-) &= \left[-2|p_D|M_B\frac{M_B-M_D}{m_b-m_c}\mathcal{R}\left(\mathbf{C_{SR}^\ell C_{TR}^{\ell*}}\right)\mathbf{F_0F_T}\right] \\
&- m_\ell\left[\frac{2|p_D|M_B\left(M_B-M_D\right)}{q^2}\mathcal{R}\left(\mathbf{C_{VR}^\ell C_{TR}^{\ell*}}\right)\mathbf{F_0F_T}\right. \\
&+ \left.\frac{|p_D|M_B\left(M_B^2-M_D^2\right)}{q^2\left(m_b-m_c\right)}\mathcal{R}\left(\mathbf{C_{SR}^\ell C_{VR}^{\ell*}}\right)\mathbf{F_0F_+}\right] \\
&- m_\ell^2\left[\frac{|p_D|M_B\left(M_B^2-M_D^2\right)}{q^4}|\mathbf{C_{VR}^\ell}|^\mathbf{2}\mathbf{F_0F_+}\right] \qquad (63) \\
\frac{1}{8}c_\ell^D(-) &= \left[\frac{4M_B^2|p_D|^2}{(M_B+M_D)^2}|\mathbf{C_{TR}^\ell}|^\mathbf{2}\mathbf{F_T^2}-\frac{M_B^2|p_D|^2}{q^2}\boxed{|\mathbf{C_{VL}^\ell}|^\mathbf{2}\mathbf{F_+^2}}\right] \\
&- m_\ell\left[\frac{4|p_D|^2M_B^2}{q^2\left(M_B+M_D\right)}\left(\mathcal{R}\left(\mathbf{C_{VL}^\ell C_{TL}^\ell}\right)\mathbf{F_+F_T}-\mathcal{R}\left(\mathbf{C_{VR}^\ell C_{TR}^{\ell*}}\right)\mathbf{F_+F_T}\right)\right] \\
&+ m_\ell^2\left[\frac{|p_D|^2M_B^2}{q^4}|\mathbf{C_{VR}^\ell}|^\mathbf{2}\mathbf{F_+^2}-\frac{4|p_D|^2M_B^2}{\left(M_B+M_D\right)^2q^2}|\mathbf{C_{TL}^\ell}|^\mathbf{2}\mathbf{F_T^2}\right]. \qquad (64)
\end{aligned}
$$

For the positive helicity of the lepton:

$$
\begin{aligned}
\frac{1}{8}a_\ell^D(+) &= \frac{M_B^2|p_D|^2}{q^2}|\mathbf{C_{VR}^\ell}|^\mathbf{2}\mathbf{F_+^2}+\frac{\left(M_B^2-M_D^2\right)^2}{4\left(m_b-m_c\right)^2}|\mathbf{C_{SL}^\ell}|^\mathbf{2}\mathbf{F_0^2} \\
&+ m_\ell\left[\frac{\left(M_B^2-M_D^2\right)^2}{2q^2(m_b-m_c)}\mathcal{R}\left(\mathbf{C_{SL}^\ell C_{VL}^{\ell*}}\right)\mathbf{F_0^2}+\frac{4M_B^2|p_D|^2}{q^2(M_B+M_D)}\mathcal{R}\left(\mathbf{C_{VR}^\ell C_{TR}^{\ell*}}\right)\mathbf{F_+F_T}\right] \\
&+ m_\ell^2\left[\frac{\left(M_B^2-M_D^2\right)^2}{4q^4}\boxed{|\mathbf{C_{VL}^\ell}|^\mathbf{2}\mathbf{F_0^2}}+\frac{4M_B^2|p_D|^2}{q^2(M_B+M_D)^2}|\mathbf{C_{TR}^\ell}|^\mathbf{2}\mathbf{F_T^2}\right] \qquad (65) \\
\frac{1}{8}b_\ell^D(+) &= \left[-2M_B|p_D|\frac{M_B-M_D}{m_b-m_c}\mathcal{R}\left(\mathbf{C_{SL}^\ell C_{TL}^{\ell*}}\right)\mathbf{F_0F_T}\right] \\
&- m_\ell\left[\frac{2|p_D|\left(M_B-M_D\right)M_B}{q^2}\mathcal{R}\left(\mathbf{C_{VL}^\ell C_{TL}^{\ell*}}\right)\mathbf{F_0F_T}\right. \\
&+ \left.\frac{|p_D|M_B\left(M_B^2-M_D^2\right)}{q^2\left(m_b-m_c\right)}\mathcal{R}\left(\mathbf{C_{SL}^\ell C_{VL}^{\ell*}}\right)\mathbf{F_0F_+}\right] \\
&- m_\ell^2\left[\frac{|p_D|M_B\left(M_B^2-M_D^2\right)}{q^4}\boxed{|\mathbf{C_{VL}^\ell}|^\mathbf{2}\mathbf{F_0F_+}}\right] \qquad (66)
\end{aligned}
$$

$$
\begin{aligned}
\frac{1}{8}c_\ell^D(+) &= \left[\frac{4|p_D|^2M_B^2}{(M_B+M_D)^2}|\mathbf{C_{TL}^\ell}|^2\mathbf{F_T^2}-\frac{|p_D|^2M_B^2}{q^2}|\mathbf{C_{VR}^\ell}|^2\mathbf{F_+^2}\right]\\
&- m_\ell\left[\frac{4|p_D|^2M_B^2}{(M_B+M_D)\,q^2}\mathcal{R}\left(\mathbf{C_{VR}^\ell C_{TR}^{\ell*}}\right)\mathbf{F_+F_T}-\frac{4M_B^2|p_D|^2}{(M_B+M_D)\,q^2}\mathcal{R}\left(\mathbf{C_{VL}^\ell C_{TL}^{\ell*}}\right)\mathbf{F_+F_T}\right]\\
&+ m_\ell^2\left[\frac{|p_D|^2M_B^2}{q^4}\boxed{|\mathbf{C_{VL}^\ell}|^2\mathbf{F_+^2}}-\frac{4|p_D|^2M_B^2}{(M_B+M_D)^2\,q^2}|\mathbf{C_{TR}^\ell}|^2\mathbf{F_T^2}\right] \qquad (67)
\end{aligned}
$$

B Full expressions for $a_\ell^{D^*}$, $b_\ell^{D^*}$ and $c_\ell^{D^*}$

$$
\begin{aligned}
a_\ell^{D^*}(-) &= \frac{8M_B^2\,|p_{D^*}|^2}{(M_B+M_{D^*})^2}\left|\mathbf{C_{VL}^\ell}\right|^2\mathbf{V^2}+\frac{(M_B+M_{D^*})^2\,(8M_{D^*}^2q^2+\lambda)}{2M_{D^*}^2q^2}\left|\mathbf{C_{AL}^\ell}\right|^2\mathbf{A_1^2}\\
&+\frac{8M_B^4|p_{D^*}|^4}{M_{D^*}^2\,(M_B+M_{D^*})^2\,q^2}\left|\mathbf{C_{AL}^\ell}\right|^2\mathbf{A_2^2}\\
&-\frac{4\,|p_{D^*}|^2\,M_B^2\,(M_B^2-M_{D^*}^2-q^2)}{M_{D^*}^2q^2}\left|\mathbf{C_{AL}^\ell}\right|^2\mathbf{A_1A_2}\\
&+\frac{32M_B^2|p_{D^*}|^2}{q^2}\left|\mathbf{C_{TR}^\ell}\right|^2\mathbf{T_1^2}+\frac{8\,(M_B^2-M_{D^*}^2)^2}{q^2}\left|\mathbf{C_{TR}^\ell}\right|^2\mathbf{T_2^2}\\
&+m_\ell\left[\frac{32M_B^2\,|p_{D^*}|^2}{q^2\,(M_B+M_{D^*})}\mathcal{R}\left(\mathbf{C_{VL}^\ell C_{TL}^{\ell*}}\right)\mathbf{VT_1}\right.\\
&+\frac{8\,(M_B+M_{D^*})\left(2M_{D^*}^2\,(M_B^2-M_{D^*}^2)+M_B^2\,|p_{D^*}|^2\right)}{q^2M_{D^*}^2}\mathcal{R}\left(\mathbf{C_{AL}^\ell C_{TL}^{\ell*}}\right)\mathbf{A_1T_2}\\
&-\frac{8M_B^2\,(M_B^2-M_{D^*}^2-q^2)\,|p_{D^*}|^2}{q^2\,(M_B-M_{D^*})\,M_{D^*}^2}\mathcal{R}\left(\mathbf{C_{AL}^\ell C_{TL}^{\ell*}}\right)\mathbf{A_1T_3}\\
&-\frac{8M_B^2\,(M_B^2+3M_{D^*}^2-q^2)\,|p_{D^*}|^2}{q^2\,(M_B+M_{D^*})\,M_{D^*}^2}\mathcal{R}\left(\mathbf{C_{AL}^\ell C_{TL}^{\ell*}}\right)\mathbf{A_2T_2}\\
&+\frac{32M_B^4|p_{D^*}|^4}{q^2M_{D^*}^2\,(M_B+M_{D^*})\,(M_B^2-M_{D^*}^2)}\mathcal{R}\left(\mathbf{C_{AL}^\ell C_{TL}^{\ell*}}\right)\mathbf{A_2T_3}\\
&+\frac{32M_B^2|p_{D^*}|^2}{(M_B+M_{D^*})q^2}\mathcal{R}\left(\mathbf{C_{VR}^\ell C_{TR}^{\ell*}}\right)\mathbf{VT_1}\\
&\left.-\frac{8(M_B-M_{D^*})(M_B+M_{D^*})^2}{q^2}\mathcal{R}\left(\mathbf{C_{AR}^\ell C_{TR}^{\ell*}}\right)\mathbf{A_1T_2}\right]\\
&+m_\ell^2\left[\frac{32M_B^2\,|p_{D^*}|^2}{q^4}\left|\mathbf{C_{TL}^\ell}\right|^2\mathbf{T_1^2}\right.
\end{aligned}
$$

$$+\frac{2\left(8M_{D^*}^2\left(2\left(M_B^2+M_{D^*}^2\right)-q^2\right)q^2+\left(4M_{D^*}^2+q^2\right)\lambda\right)}{q^4M_{D^*}^2}\left|\mathbf{C_{TL}^{\ell}}\right|^2\mathbf{T_2^2}$$
$$+\frac{32M_B^4|p_{D^*}|^4}{q^2M_{D^*}^2\left(M_B^2-M_{D^*}^2\right)^2}\left|\mathbf{C_{TL}^{\ell}}\right|^2\mathbf{T_3^2}-\frac{16M_B^2\left|p_{D^*}\right|^2\left(M_B^2+3M_{D^*}^2-q^2\right)}{q^2M_{D^*}^2\left(M_B^2-M_{D^*}^2\right)}\left|\mathbf{C_{TL}^{\ell}}\right|^2\mathbf{T_2T_3}\Bigg] \quad (68)$$

$$\begin{aligned}
b_\ell^{D^*}(-) &= -16|p_{D^*}|M_B\mathcal{R}\left(\mathbf{C_{VL}^{\ell}C_{AL}^{\ell *}}\right)\mathbf{VA_1}\\
&+\frac{32M_B^3|p_{D^*}|^3}{(m_b+m_c)(M_B^2-M_{D^*}^2)M_{D^*}}\mathcal{R}\left(\mathbf{C_{PR}^{\ell}C_{TR}^{\ell *}}\right)\mathbf{A_0T_3}\\
&-\frac{8M_B|p_{D^*}|\left(M_B^2+3M_{D^*}^2-q^2\right)}{(m_b+m_c)M_{D^*}}\mathcal{R}\left(\mathbf{C_{PR}^{\ell}C_{TR}^{\ell *}}\right)\mathbf{A_0T_2}\\
&-m_\ell\Bigg[\frac{32M_B\left(M_B-M_{D^*}\right)|p_{D^*}|}{q^2}\mathcal{R}\left(\mathbf{C_{VL}^{\ell}C_{TL}^{\ell *}}\right)\mathbf{VT_2}\\
&+\frac{32M_B\left(M_B+M_{D^*}\right)|p_{D^*}|}{q^2}\mathcal{R}\left(\mathbf{C_{AL}^{\ell}C_{TL}^{\ell *}}\right)\mathbf{A_1T_1}\\
&+\frac{8M_B|p_{D^*}|\left(M_B^2+3M_{D^*}^2-q^2\right)}{M_{D^*}q^2}\mathcal{R}\left(\mathbf{C_{AR}^{\ell}C_{TR}^{\ell *}}\right)\mathbf{A_0T_2}\\
&-\frac{32M_B^3|p_{D^*}|^3}{(M_B-M_{D^*})M_{D^*}(M_B+M_{D^*})q^2}\mathcal{R}\left(\mathbf{C_{AR}^{\ell}C_{TR}^{\ell *}}\right)\mathbf{A_0T_3}\Bigg]\\
&-m_\ell^2\left[\frac{64M_B\left(M_B^2-M_{D^*}^2\right)|p_{D^*}|}{q^4}\left|\mathbf{C_{TL}^{\ell}}\right|^2\mathbf{T_1T_2}\right] \qquad (69)
\end{aligned}$$

$$\begin{aligned}
c_\ell^{D^*}(-) &= \frac{8\left|p_{D^*}\right|^2M_B^2}{\left(M_B+M_{D^*}\right)^2}\left|\mathbf{C_{VL}^{\ell}}\right|^2\mathbf{V^2}-\frac{\left(M_B+M_{D^*}\right)^2\lambda}{2M_{D^*}^2q^2}\left|\mathbf{C_{AL}^{\ell}}\right|^2\mathbf{A_1^2}\\
&-\frac{8|p_{D^*}|^4M_B^4}{\left(M_B+M_{D^*}\right)^2M_{D^*}^2q^2}\left|\mathbf{C_{AL}^{\ell}}\right|^2\mathbf{A_2^2}\\
&+\frac{4\left|p_{D^*}\right|^2M_B^2\left(M_B^2-M_{D^*}^2-q^2\right)}{M_{D^*}^2q^2}\left|\mathbf{C_{AL}^{\ell}}\right|^2\mathbf{A_1A_2}\\
&-\frac{32M_B^2M_{D^*}^2\left(M_B^2-M_{D^*}^2\right)^2\left|p_{D^*}\right|^2}{\left(-M_B^2M_{D^*}+M_{D^*}^3\right)^2q^2}\left|\mathbf{C_{TR}^{\ell}}\right|^2\mathbf{T_1^2}\\
&\frac{2\left(M_B^2-M_{D^*}^2\right)^2}{M_{D^*}^2}\left|\mathbf{C_{TR}^{\ell}}\right|^2\mathbf{T_2^2}\\
&-\frac{4\left(-M_B^2+M_{D^*}^2\right)\left(-M_B^4+M_{D^*}^4+4M_B^2|p_{D^*}|^2\right)}{M_{D^*}^2q^2}\left|\mathbf{C_{TR}^{\ell}}\right|^2\mathbf{T_2^2}\\
&+\frac{32M_B^4|p_{D^*}|^4}{\left(-M_B^2M_{D^*}+M_{D^*}^3\right)^2}\left|\mathbf{C_{TR}^{\ell}}\right|^2\mathbf{T_3^2}
\end{aligned}$$

$$
\begin{aligned}
&+\frac{16M_B^2|p_{D^*}|^2\left(M_B^2+3M_{D^*}^2-q^2\right)}{-M_B^2M_{D^*}^2+M_{D^*}^4}\left|\mathbf{C_{TR}^{\ell}}\right|^{\mathbf{2}}\mathbf{T_2T_3}\\
&+m_\ell\left[\frac{32M_B^2\left|p_{D^*}\right|^2}{q^2\left(M_B+M_{D^*}\right)}\mathcal{R}\left(\mathbf{C_{VL}^{\ell}C_{TL}^{\ell*}}\right)\mathbf{VT_1}\right.\\
&-\frac{8M_B^2\left(M_B+M_{D^*}\right)\left|p_{D^*}\right|^2}{q^2M_{D^*}^2}\mathcal{R}\left(\mathbf{C_{AL}^{\ell}C_{TL}^{\ell*}}\right)\mathbf{A_1T_2}\\
&+\frac{8M_B^2\left(M_B^2-M_{D^*}^2-q^2\right)\left|p_{D^*}\right|^2}{q^2M_{D^*}^2\left(M_B-M_{D^*}\right)}\mathcal{R}\left(\mathbf{C_{AL}^{\ell}C_{TL}^{\ell*}}\right)\mathbf{A_1T_3}\\
&+\frac{8M_B^2\left(M_B^2+3M_{D^*}^2-q^2\right)\left|p_{D^*}\right|^2}{q^2M_{D^*}^2\left(M_B+M_{D^*}\right)}\mathcal{R}\left(\mathbf{C_{AL}^{\ell}C_{TL}^{\ell*}}\right)\mathbf{A_2T_2}\\
&-\frac{32M_B^4|p_{D^*}|^4}{q^2M_{D^*}^2\left(M_B+M_{D^*}\right)\left(M_B^2-M_{D^*}^2\right)}\mathcal{R}\left(\mathbf{C_{AL}^{\ell}C_{TL}^{\ell*}}\right)\mathbf{A_2T_3}\\
&-\frac{32M_B^2|p_{D^*}|^2}{\left(M_B+M_{D^*}\right)q^2}\mathcal{R}\left(\mathbf{C_{VR}^{\ell}C_{TR}^{\ell*}}\right)\mathbf{VT_1}\\
&+\frac{8M_B^2(M_B+M_{D^*})|p_{D^*}|^2}{M_{D^*}^2q^2}\mathcal{R}\left(\mathbf{C_{AR}^{\ell}C_{TR}^{\ell*}}\right)\mathbf{A_1T_2}\\
&-\frac{8M_B^2|p_{D^*}|^2\left(-M_B^2+M_{D^*}^2+q^2\right)}{(M_B-M_{D^*})M_{D^*}^2q^2}\mathcal{R}\left(\mathbf{C_{VR}^{\ell}C_{TR}^{\ell*}}\right)\mathbf{A_1T_3}\\
&+\frac{8M_B^2|p_{D^*}|^2\left(M_B^2+3M_{D^*}^2-q^2\right)}{M_{D^*}^2(M_B+M_{D^*})q^2}\mathcal{R}\left(\mathbf{C_{VR}^{\ell}C_{TR}^{\ell*}}\right)\mathbf{A_2T_2}\\
&\left.-\frac{32M_B^4|p_{D^*}|^4}{(M_B-M_{D^*})M_{D^*}^2(M_B+M_{D^*})^2q^2}\mathcal{R}\left(\mathbf{C_{VR}^{\ell}C_{TR}^{\ell*}}\right)\mathbf{A_2T_3}\right]\\
&+m_\ell^2\left[\frac{32M_B^2\left|p_{D^*}\right|^2}{q^4}\left|\mathbf{C_{TL}^{\ell}}\right|^{\mathbf{2}}\mathbf{T_1^2}+\frac{2\left(4M_{D^*}^2-q^2\right)\lambda}{M_{D^*}^2q^4}\left|\mathbf{C_{TL}^{\ell}}\right|^{\mathbf{2}}\mathbf{T_2^2}\right.\\
&-\frac{32M_B^4|p_{D^*}|^4}{q^2M_{D^*}^2\left(M_B^2-M_{D^*}^2\right)^2}\left|\mathbf{C_{TL}^{\ell}}\right|^{\mathbf{2}}\mathbf{T_3^2}\\
&\left.+\frac{16M_B^2\left|p_{D^*}\right|^2\left(M_B^2+3M_{D^*}^2-q^2\right)}{q^2M_{D^*}^2\left(M_B^2-M_{D^*}^2\right)}\left|\mathbf{C_{TL}^{\ell}}\right|^{\mathbf{2}}\mathbf{T_2T_3}\right] \qquad (70)
\end{aligned}
$$

$$
\begin{aligned}
a_\ell^{D^*}(+) \;=\;& \frac{8\left|p_{D^*}\right|^2M_B^2}{\left(m_b+m_c\right)^2}\left|\mathbf{C_{PL}^{\ell}}\right|^{\mathbf{2}}\mathbf{A_0^2}+\frac{32M_B^2\left|p_{D^*}\right|^2}{q^2}\left|\mathbf{C_{TL}^{\ell}}\right|^{\mathbf{2}}\mathbf{T_1^2}+\frac{8\left(M_B^2-M_{D^*}^2\right)^2}{q^2}\left|\mathbf{C_{TL}^{\ell}}\right|^{\mathbf{2}}\mathbf{T_2^2}\\
&-m_\ell\left[\frac{16\left|p_{D^*}\right|^2M_B^2}{\left(m_b+m_c\right)q^2}\mathcal{R}\left(\mathbf{C_{AL}^{\ell}C_{PL}^{\ell*}}\right)\mathbf{A_0^2}\right.
\end{aligned}
$$

$$
\begin{aligned}
&-\frac{32M_B^2\left|p_{D^*}\right|^2}{q^2\left(M_B+M_{D^*}\right)}\mathcal{R}\left(\mathbf{C_{VL}^{\ell}C_{TL}^{\ell *}}\right)\mathbf{VT_1}\\
&-\frac{8(M_B+M_{D^*})\left(M_B^2-M_{D^*}^2\right)}{q^2}\mathcal{R}\left(\mathbf{C_{AL}^{\ell}C_{TL}^{\ell *}}\right)\mathbf{A_1T_2}\\
&-\frac{32M_B^2|p_{D^*}|^2}{(M_B+M_{D^*})q^2}\mathcal{R}\left(\mathbf{C_{VR}^{\ell}C_{TR}^{\ell *}}\right)\mathbf{VT_1}\\
&+\frac{8(M_B+M_{D^*})\left(-2M_{D^*}^4+M_B^2\left(2M_{D^*}^2+|p_{D^*}|^2\right)\right)}{M_{D^*}^2q^2}\mathcal{R}\left(\mathbf{C_{AR}^{\ell}C_{TR}^{\ell *}}\right)\mathbf{A_1T_2}\\
&+\frac{8M_B^2|p_{D^*}|^2\left(-M_B^2+M_{D^*}^2+q^2\right)}{(M_B-M_{D^*})M_{D^*}^2q^2}\mathcal{R}\left(\mathbf{C_{AR}^{\ell}C_{TR}^{\ell *}}\right)\mathbf{A_1T_3}\\
&-\frac{8M_B^2|p_{D^*}|^2\left(M_B^2+3M_{D^*}^2-q^2\right)}{M_{D^*}^2(M_B+M_{D^*})q^2}\mathcal{R}\left(\mathbf{C_{AR}^{\ell}C_{TR}^{\ell *}}\right)\mathbf{A_2T_2}\\
&+\frac{32M_B^4|p_{D^*}|^4}{(M_B-M_{D^*})M_{D^*}^2(M_B+M_{D^*})^2q^2}\mathcal{R}\left(\mathbf{C_{AR}^{\ell}C_{TR}^{\ell *}}\right)\mathbf{A_2T_3}\Bigg]\\
&+m_\ell^2\Bigg[\frac{8\left|p_{D^*}\right|^2M_B^2}{q^4}\left|\mathbf{C_{AL}^{\ell}}\right|^2\mathbf{A_0^2}+\frac{8\left|p_{D^*}\right|^2M_B^2}{\left(M_B+M_{D^*}\right)^2q^2}\left|\mathbf{C_{VL}^{\ell}}\right|^2\mathbf{V^2}\\
&\quad+\frac{2\left(M_B+M_{D^*}\right)^2}{q^2}\left|\mathbf{C_{AL}^{\ell}}\right|^2\mathbf{A_1^2}\\
&+\frac{32M_B^2|p_{D^*}|^2}{q^4}\left|\mathbf{C_{TR}^{\ell}}\right|^2\mathbf{T_1^2}+8\frac{M_B^2|p_{D^*}|^2}{M_{D^*}^2q^2}\left|\mathbf{C_{TR}^{\ell}}\right|^2\mathbf{T_2^2}\\
&+\frac{16\left(M_B^4+M_{D^*}^4-2M_B^2\left(M_{D^*}^2+|p_{D^*}|^2\right)\right)}{q^4}\left|\mathbf{C_{TR}^{\ell}}\right|^2\mathbf{T_2^2}\\
&+\frac{32M_B^4|p_{D^*}|^4}{\left(-M_B^2M_{D^*}+M_{D^*}^3\right)^2q^2}\left|\mathbf{C_{TR}^{\ell}}\right|^2\mathbf{T_3^2}\\
&+\frac{16M_B^2|p_{D^*}|^2\left(M_B^2+3M_{D^*}^2-q^2\right)}{M_{D^*}^2\left(-M_B^2+M_{D^*}^2\right)q^2}\left|\mathbf{C_{TR}^{\ell}}\right|^2\mathbf{T_2T_3}\Bigg]
\end{aligned}
\tag{71}
$$

$$
\begin{aligned}
b_\ell^{D^*}(+) \;=\;& \frac{8M_B\left(M_B^2+3M_{D^*}^2-q^2\right)|p_{D^*}|}{\left(m_b+m_c\right)M_{D^*}}\mathcal{R}\left(\mathbf{C_{PL}^{\ell}C_{TL}^{\ell *}}\right)\mathbf{A_0T_2}\\
&-\frac{32M_B^3|p_{D^*}|^3}{\left(m_b+m_c\right)M_{D^*}\left(M_B^2-M_{D^*}^2\right)}\mathcal{R}\left(\mathbf{C_{PL}^{\ell}C_{TL}^{\ell *}}\right)\mathbf{A_0T_3}\\
&+m_\ell\Bigg[\frac{4|p_{D^*}|M_B\left(M_B+M_{D^*}\right)\left(M_B^2-M_{D^*}^2-q^2\right)}{M_{D^*}\left(m_b+m_c\right)q^2}\mathcal{R}\left(\mathbf{C_{AL}^{\ell}C_{PL}^{\ell *}}\right)\mathbf{A_0A_1}\\
&-\frac{16}{\left(m_b+m_c\right)}\frac{|p_{D^*}|^3M_B^3}{\left(M_B+M_{D^*}\right)M_{D^*}q^2}\mathcal{R}\left(\mathbf{C_{AL}^{\ell}C_{PL}^{\ell *}}\right)\mathbf{A_0A_2}
\end{aligned}
$$

$$
\begin{aligned}
&-\frac{8M_B\left(M_B^2+3M_{D^*}^2-q^2\right)|p_{D^*}|}{M_{D^*}q^2}\mathcal{R}\left(\mathbf{C_{AL}^{\ell}C_{TL}^{\ell *}}\right)\mathbf{A_0T_2}\\
&+\frac{32M_B^3|p_{D^*}|^3}{q^2M_{D^*}\left(M_B^2-M_{D^*}^2\right)}\mathcal{R}\left(\mathbf{C_{AL}^{\ell}C_{TL}^{\ell *}}\right)\mathbf{A_0T_3}\\
&+\frac{32M_B(-M_B+M_{D^*})|p_{D^*}|}{q^2}\mathcal{R}\left(\mathbf{C_{VR}^{\ell}C_{TR}^{\ell *}}\right)\mathbf{VT_2}\\
&+\frac{32M_B(M_B+M_{D^*})|p_{D^*}|}{q^2}\mathcal{R}\left(\mathbf{C_{AR}^{\ell}C_{TR}^{\ell *}}\right)\mathbf{A_1T_1}\Bigg]\\
&+m_\ell^2\Bigg[-\frac{4|p_{D^*}|M_B\left(M_B+M_{D^*}\right)}{M_{D^*}q^4}\left(M_B^2-M_{D^*}^2-q^2\right)\left|\mathbf{C_{AL}^{\ell}}\right|^{\mathbf{2}}\mathbf{A_0A_1}\\
&+\frac{16|p_{D^*}|^3M_B^3}{\left(M_B+M_{D^*}\right)M_{D^*}q^4}\left|\mathbf{C_{AL}^{\ell}}\right|^{\mathbf{2}}\mathbf{A_0A_2}\\
&+\frac{64M_B\left(-M_B^2+M_{D^*}^2\right)|p_{D^*}|}{q^4}\left|\mathbf{C_{TR}^{\ell}}\right|^{\mathbf{2}}\mathbf{T_1T_2}\Bigg]
\end{aligned}
\tag{72}
$$

$$
\begin{aligned}
c_\ell^{D^*}(+) \;=\; &-\frac{32M_B^2\left|p_{D^*}\right|^2}{q^2}\left|\mathbf{C_{TL}^{\ell}}\right|^{\mathbf{2}}\mathbf{T_1^2}-\frac{2\left(4M_{D^*}^2-q^2\right)\lambda}{M_{D^*}^2q^2}\left|\mathbf{C_{TL}^{\ell}}\right|^{\mathbf{2}}\mathbf{T_2^2}+\frac{32M_B^4|p_{D^*}|^4}{M_{D^*}^2\left(M_B^2-M_{D^*}^2\right)^2}\left|\mathbf{C_{TL}^{\ell}}\right|^{\mathbf{2}}\mathbf{T_3^2}\\
&-\frac{16M_B^2\left|p_{D^*}\right|^2\left(M_B^2+3M_{D^*}^2-q^2\right)}{M_{D^*}^2\left(M_B^2-M_{D^*}^2\right)}\left|\mathbf{C_{TL}^{\ell}}\right|^{\mathbf{2}}\mathbf{T_2T_3}\\
&-m_\ell\Bigg[\frac{32M_B^2\left|p_{D^*}\right|^2}{q^2\left(M_B+M_{D^*}\right)}\mathcal{R}\left(\mathbf{C_{VL}^{\ell}C_{TL}^{\ell *}}\right)\mathbf{VT_1}\\
&-\frac{8M_B^2\left(M_B+M_{D^*}\right)\left|p_{D^*}\right|^2}{q^2M_{D^*}^2}\mathcal{R}\left(\mathbf{C_{AL}^{\ell}C_{TL}^{\ell *}}\right)\mathbf{A_1T_2}\\
&+\frac{8M_B^2\left(M_B^2-M_{D^*}^2-q^2\right)\left|p_{D^*}\right|^2}{q^2M_{D^*}^2\left(M_B-M_{D^*}\right)}\mathcal{R}\left(\mathbf{C_{AL}^{\ell}C_{TL}^{\ell *}}\right)\mathbf{A_1T_3}\\
&+\frac{8M_B^2\left(M_B^2+3M_{D^*}^2-q^2\right)\left|p_{D^*}\right|^2}{q^2M_{D^*}^2\left(M_B+M_{D^*}\right)}\mathcal{R}\left(\mathbf{C_{AL}^{\ell}C_{TL}^{\ell *}}\right)\mathbf{A_2T_2}\\
&-\frac{32M_B^4|p_{D^*}|^4}{q^2M_{D^*}^2\left(M_B+M_{D^*}\right)\left(M_B^2-M_{D^*}^2\right)}\mathcal{R}\left(\mathbf{C_{AL}^{\ell}C_{TL}^{\ell *}}\right)\mathbf{A_2T_3}\\
&+\frac{32M_B^2|p_{D^*}|^2}{(M_B+M_{D^*})q^2}\mathcal{R}\left(\mathbf{C_{VR}^{\ell}C_{TR}^{\ell *}}\right)\mathbf{VT_1}\\
&+\frac{8M_B^2(M_B+M_{D^*})|p_{D^*}|^2}{M_{D^*}^2q^2}\mathcal{R}\left(\mathbf{C_{AR}^{\ell}C_{TR}^{\ell *}}\right)\mathbf{A_1T_2}\\
&-\frac{8M_B^2|p_{D^*}|^2\left(-M_B^2+M_{D^*}^2+q^2\right)}{(M_B-M_{D^*})M_{D^*}^2q^2}\mathcal{R}\left(\mathbf{C_{AR}^{\ell}C_{TR}^{\ell *}}\right)\mathbf{A_1T_3}
\end{aligned}
\tag{73}
$$

$$
\begin{aligned}
&+\frac{8M_B^2|p_{D^*}|^2\left(M_B^2+3M_{D^*}^2-q^2\right)}{M_{D^*}^2(M_B+M_{D^*})q^2}\mathcal{R}\left(\mathbf{C_{AR}^{\ell}C_{TR}^{\ell *}}\right)\mathbf{A_2T_2}\\
&-\frac{32M_B^4|p_{D^*}|^4}{(M_B-M_{D^*})M_{D^*}^2(M_B+M_{D^*})^2q^2}\mathcal{R}\left(\mathbf{C_{AR}^{\ell}C_{TR}^{\ell *}}\right)\mathbf{A_2T_3}\Bigg]\\
&+m_\ell^2\Bigg[-\frac{8\left|p_{D^*}\right|^2M_B^2}{\left(M_B+M_{D^*}\right)^2q^2}\left|\mathbf{C_{VL}^{\ell}}\right|^2\mathbf{V^2}+\frac{\left(M_B+M_{D^*}\right)^2\lambda}{2M_{D^*}^2q^4}\left|\mathbf{C_{AL}^{\ell}}\right|^2\mathbf{A_1^2}\\
&+\frac{8|p_{D^*}|^4M_B^4}{M_{D^*}^2\left(M_B+M_{D^*}\right)^2q^4}\left|\mathbf{C_{AL}^{\ell}}\right|^2\mathbf{A_2^2}\\
&-\frac{4\left|p_{D^*}\right|^2M_B^2}{M_{D^*}^2q^4}\left(M_B^2-M_{D^*}^2-q^2\right)\left|\mathbf{C_{AL}^{\ell}}\right|^2\mathbf{A_1A_2}\\
&+\frac{32M_B^2|p_{D^*}|^2}{q^4}\left|\mathbf{C_{TR}^{\ell}}\right|^2\mathbf{T_1^2}+\frac{8M_B^2|p_{D^*}|^2\left(4M_{D^*}^2-q^2\right)}{M_{D^*}^2q^4}\left|\mathbf{C_{TR}^{\ell}}\right|^2\mathbf{T_2^2}\\
&-\frac{32M_B^4|p_{D^*}|^4}{\left(-M_B^2M_{D^*}+M_{D^*}^3\right)^2q^2}\left|\mathbf{C_{TR}^{\ell}}\right|^2\mathbf{T_3^2}\\
&+\frac{16M_B^2|p_{D^*}|^2\left(M_B^2+3M_{D^*}^2-q^2\right)}{M_{D^*}^2\left(M_B^2-M_{D^*}^2\right)q^2}\left|\mathbf{C_{TR}^{\ell}}\right|^2\mathbf{T_2T_3}\Bigg]
\end{aligned}
\tag{74}
$$

C Contribution of the Tensor operator $\mathcal{O}_{\rm TL}^{cb\ell}$

C.1 $\overline{B}\to D\tau\bar{\nu}_\tau$

C_{TL}^τ	$P_\tau(D)$	R_D [bin]			
$\in$ [0.240, 0.796]	$\in$ [0.125, 0.254]	$[m_\tau^2-5]$ GeV^2	$[5-7]$ GeV^2	$[7-9]$ GeV^2	$[9-(M_B-M_D)^2]$ GeV^2
C_{TL}^τ	$\mathcal{A}_{FB}^D$	[0.178, 0.233]	[0.673, 0.907]	[1.135, 1.533]	[1.989, 2.508]
$\in$ [-3.500, -3.052]	$\in [-0.451, -0.404]$				

Table 7: Predictions for $P_\tau(D)$, $\mathcal{A}_{FB}^D$ and binwise values of R_D for a range of C_{TL}^τ for which R_D is experimentally satisfied within 1σ. The range of the WCs is given in the first column. The values in the subsequent columns are only for the range of C_{TL}^τ closest to the SM value of 0, viz. the positive range.

In this section we investigate the effect of the tensor operator $\mathcal{O}_{\rm TL}^{cb\ell}$ on the $\overline{B}\to D\tau\bar{\nu}_\tau$ decay. In the first row of table 7, we show the range of C_{TL}^τ that explains R_D within 1σ. In the subsequent rows, we show the predictions of $P_\tau(D)$, $\mathcal{A}_{FB}^D$ and binwise R_D for the allowed range of C_{TL}^τ that is closest to zero (i.e., $C_{TL}^\tau\in[0.240,\,0.796]$). A comparison with the left plot of Fig. 6 reveals that $P_\tau(D)$ in this case is quite different from the other cases and thus, can completely distinguish the tensor operator from the vector or scalar operators. Similarly, $\mathcal{A}_{FB}^D$ can also be used to distinguish the tensor from the vector operator, however, there exists some degeneracy with the scalar operator.

The variation of R_D as a function of C_{TL}^{τ} is also shown in the left plot of Fig. 11. The predictions for binwise R_D for the tensor operators are graphically presented in the right plot of Fig. 11.

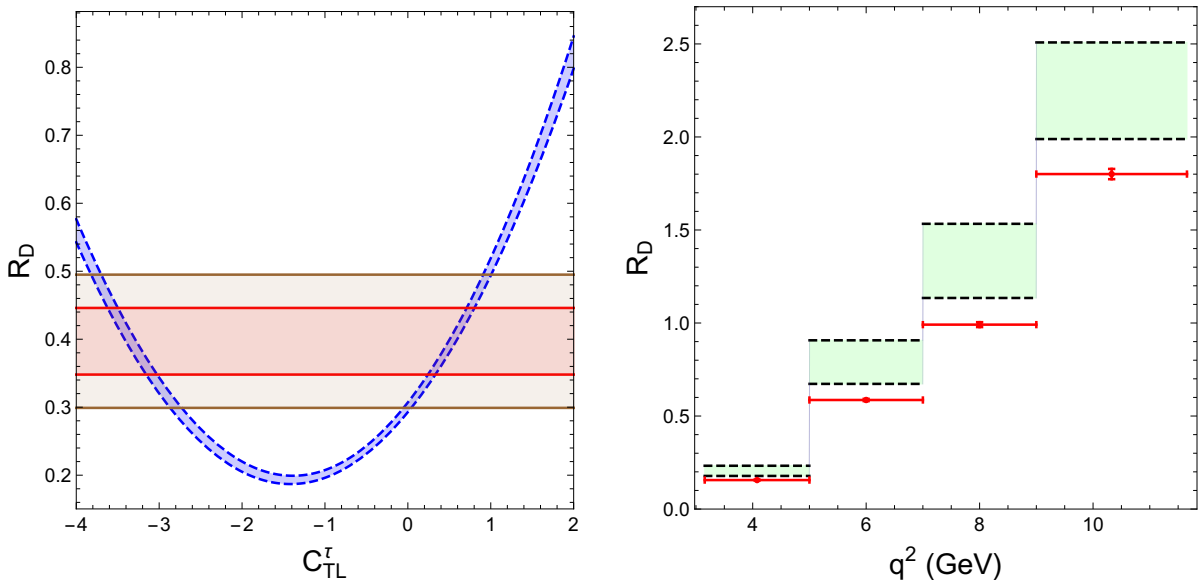

Figure 11: The left panel shows the dependence of R_D with respect to the variation of the WCs C_{TL}^{τ} and the right panel shows the prediction for R_D in four different bins of q^2 from table 7.

C.2 $\overline{B} \to D^* \tau \bar{\nu}_\tau$

C_{TL}^{τ}	$P_\tau(D^*)$	R_{D^*} [bin]			
$\in$ [-0.120, -0.058]	$\in$ [-0.481, -0.441]	$[m_\tau^2 - 5]$ GeV^2	$[5-7]$ GeV^2	$[7-9]$ GeV^2	$[9-(M_B - M_{D^*})^2]$ GeV^2
C_{TL}^{τ} $\in$ [0.709, 0.834]	$\mathcal{A}_{FB}^{D^*}$ $\in$ [−0.016, 0.034]	[0.113, 0.129]	[0.368, 0.423]	[0.531, 0.610]	[0.620, 0.715]

Table 8: Predictions for $P_\tau(D^*)$, $\mathcal{A}_{FB}^{D^*}$ and binwise values of R_{D^*} for a range of C_{TL}^{τ} for which R_{D^*} is experimentally satisfied within 1σ. The corresponding range of the WCs is given in the first column. The values in the subsequent columns are only for the range of C_{TL}^{τ} closest to the SM value of 0, viz. the positive range.

The range of C_{TL}^{τ} that explains R_D^* within 1σ is shown in the first column of table 8. The resulting values for $P_\tau(D^*)$, $\mathcal{A}_{FB}^{D^*}$ and binwise R_D^* are shown in the subsequent columns. In the left plot of Fig. 12 we also show the dependence of R_D^* as a function of C_{TL}^{τ}. The right plot shows the binwise R_D^* graphically.

A quick look at the allowed ranges for C_{TL} in the $B \to D$ (Table 7) and the $B \to D^*$ (Table 8) cases shows that there is a region of overlap, around 0.7-0.8, which allows one to explain both the anomalies simultaneously.

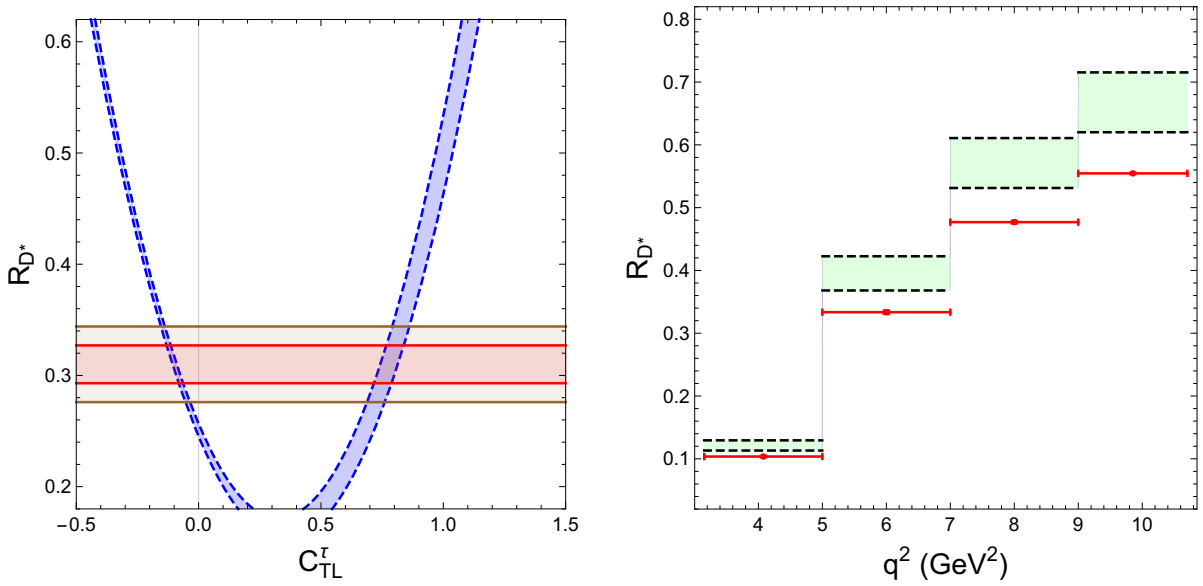

Figure 12: The left panel shows the dependence of R_{D^*} with respect to the variation of the WCs C^{τ}_{TL} and the right panel shows the prediction for R_{D^*} in four different bins of q^2 from table 8.

D $\mathrm{SU(3)_C \times SU(2)_L \times U(1)_Y}$ gauge invariance

In table 9 we show how the WCs of the operators in this paper are related to the WCs of the gauge invariant dimension 6 operators of [64]. We use the following set of notations:

- Greek letters $\mu, \nu, \cdots$ are used to denote Lorentz indices.
- SU(2) fundamental indices are denoted by $a, b, \cdots$ and $I, J \cdots$ will be used to denote adjoint indices.
- To represent quark (lepton) flavors, we use $i, j, k \cdots$ $(m, n \cdots)$.
- A tilde (e.g. $\tilde{\mathcal{C}}$) is used to denote high energy Wilson coefficients.
- The notation for the operators is as given in [64].

- definition of the quark mixing matrices (f and m denote flavour and mass bases)

$$u_L^f = V_L^u u_L^m \tag{75}$$
$$u_R^f = V_R^u u_R^m \tag{76}$$
$$d_L^f = V_L^d d_L^m \tag{77}$$
$$d_R^f = V_R^d d_R^m \tag{78}$$

WCs in this work				WCs in [64]	Operator structure
$\frac{2G_F V_{cb}}{\sqrt{2}} \times$	$\Delta C_9^{cb\tau *} = -\Delta C_{10}^{cb\tau *}$		=	$\frac{1}{2}[V_L^{d\,\dagger}]_{3i}\left[-\frac{g^2 v^2}{2M_W^2}\left(\tilde{C}_{\phi q}^{(3)ij,33\,\dagger} + \tilde{C}_{\phi \ell}^{(3)33,ij}\right) + 2\tilde{C}_{\ell q}^{(3)ij\,33}\right][V_L^u]_{j2}$	$\left[\bar{q}_i^2\gamma^\mu q_j^1\right]\left[\bar{\ell}_3^1\gamma_\mu \ell_3^2\right]$ $[\phi^\dagger i\overleftrightarrow{D}^I_\mu \phi][\bar{\ell}_i^1 \frac{\sigma^I}{2}\gamma^\mu \ell_j^2]$ $[\phi^\dagger i\overleftrightarrow{D}^I_\mu \phi][\bar{q}_i^2 \frac{\sigma^I}{2}\gamma^\mu q_j^1]$
	$C_9^{cb\tau\,\prime *} = -C_{10}^{cb\tau\,\prime *}$		=	$-\frac{1}{2}[V_R^{u\,\dagger}]_{2i}\frac{g^2 v^2}{2M_W^2}\tilde{C}_{\phi ud}^{ij\,33\,\dagger}[V_R^d]_{j3}$	$\left[\bar{d}_i\gamma^\mu u_j\right]\left[\bar{\ell}_3^1\gamma_\mu \ell_3^2\right]$
	$C_s^{cb\tau *} = -C_p^{cb\tau *}$		=	$\frac{1}{2}[V_L^{d\,\dagger}]_{3i}\,\tilde{C}_{\ell equ}^{(1)ij,33}[V_R^u]_{j2}$	$\left(\bar{\ell}_3^1 e_3\right)\left(\bar{q}_i^2 u_j\right)$
	$C_s^{cb\tau\,\prime *} = -C_p^{cb\tau\,\prime *}$		=	$\frac{1}{2}[V_R^{d\,\dagger}]_{3i}\,\tilde{C}_{\ell edq}^{ij,33}[V_L^u]_{j2}$	$\left(\bar{\ell}_3^1 e_3\right)\left(\bar{d}_i q_j^1\right)$
	$C_T^{cb\tau *} = -C_{T5}^{cb\tau *}$		=	$\frac{1}{2}[V_L^{d\,\dagger}]_{3i}\,\tilde{C}_{\ell equ}^{(3)ij,33}\,[V_R^u]_{j2}$	$\left(\bar{\ell}_3^1\sigma_{\mu\nu} e_3\right)\epsilon_{12}\left(\bar{q}_i^2\sigma^{\mu\nu} u_j\right)$

Table 9: Correspondence of our operators with those in reference [64]. The mixing of different lepton flavours are ignored.

References

[1] LHCb collaboration, R. Aaij et al., *Test of lepton universality using $B^+ \to K^+\ell^+\ell^-$ decays*, *Phys. Rev. Lett.* **113** (2014) 151601, [1406.6482].

[2] LHCb collaboration, R. Aaij et al., *Angular analysis of the $B^0 \to K^{*0}\mu^+\mu^-$ decay using 3 fb^{-1} of integrated luminosity*, *JHEP* **02** (2016) 104, [1512.04442].

[3] W. Altmannshofer, P. Ball, A. Bharucha, A. J. Buras, D. M. Straub and M. Wick, *Symmetries and Asymmetries of $B \to K^*\mu^+\mu^-$ Decays in the Standard Model and Beyond*, *JHEP* **01** (2009) 019, [0811.1214].

[4] A. K. Alok, A. Dighe, D. Ghosh, D. London, J. Matias, M. Nagashima et al., *New-physics contributions to the forward-backward asymmetry in $B \to K^*\mu^+\mu^-$*, *JHEP* **02** (2010) 053, [0912.1382].

[5] A. K. Alok, A. Datta, A. Dighe, M. Duraisamy, D. Ghosh and D. London, *New Physics in $b \to s\mu^+\mu^-$: CP-Conserving Observables*, *JHEP* **11** (2011) 121, [1008.2367].

[6] A. K. Alok, A. Datta, A. Dighe, M. Duraisamy, D. Ghosh and D. London, *New Physics in $b \to s\mu^+\mu^-$: CP-Violating Observables*, *JHEP* **11** (2011) 122, [1103.5344].

[7] S. Descotes-Genon, D. Ghosh, J. Matias and M. Ramon, *Exploring New Physics in the C7-C7' plane*, *JHEP* **06** (2011) 099, [1104.3342].

[8] S. Descotes-Genon, J. Matias and J. Virto, *Understanding the $B \to K^*\mu^+\mu^-$ Anomaly*, *Phys. Rev.* **D88** (2013) 074002, [1307.5683].

[9] W. Altmannshofer and D. M. Straub, *New physics in $B \to K^*\mu\mu$?*, *Eur. Phys. J.* **C73** (2013) 2646, [1308.1501].

[10] A. Datta, M. Duraisamy and D. Ghosh, *Explaining the $B \to K^*\mu^+\mu^-$ data with scalar interactions*, *Phys. Rev.* **D89** (2014) 071501, [1310.1937].

[11] D. Ghosh, M. Nardecchia and S. A. Renner, *Hint of Lepton Flavour Non-Universality in B Meson Decays*, *JHEP* **12** (2014) 131, [1408.4097].

[12] R. Mandal, R. Sinha and D. Das, *Testing New Physics Effects in $B \to K^*\ell^+\ell^-$*, *Phys. Rev.* **D90** (2014) 096006, [1409.3088].

[13] W. Altmannshofer and D. M. Straub, *New physics in $b \to s$ transitions after LHC run 1*, *Eur. Phys. J.* **C75** (2015) 382, [1411.3161].

[14] S. Jager and J. Martin Camalich, *Reassessing the discovery potential of the $B \to K^*\ell^+\ell^-$ decays in the large-recoil region: SM challenges and BSM opportunities*, *Phys. Rev.* **D93** (2016) 014028, [1412.3183].

[15] S. Descotes-Genon, L. Hofer, J. Matias and J. Virto, *Global analysis of $b \to s\ell\ell$ anomalies*, *JHEP* **06** (2016) 092, [1510.04239].

[16] M. Ciuchini, M. Fedele, E. Franco, S. Mishima, A. Paul, L. Silvestrini et al., *$B \to K^*\ell^+\ell^-$ decays at large recoil in the Standard Model: a theoretical reappraisal*, *JHEP* **06** (2016) 116, [1512.07157].

[17] Heavy Flavor Averaging Group (HFAG) collaboration, Y. Amhis et al., *Averages of b-hadron, c-hadron, and τ-lepton properties as of summer 2014*, 1412.7515.

[18] Belle collaboration, M. Huschle et al., *Measurement of the branching ratio of $\bar{B} \to D^{(*)}\tau^-\bar{\nu}_\tau$ relative to $\bar{B} \to D^{(*)}\ell^-\bar{\nu}_\ell$ decays with hadronic tagging at Belle*, *Phys. Rev.* **D92** (2015) 072014, [1507.03233].

[19] MILC collaboration, J. A. Bailey et al., *$B \to D\ell\nu$ form factors at nonzero recoil and $|V_{cb}|$ from 2+1-flavor lattice QCD*, *Phys. Rev.* **D92** (2015) 034506, [1503.07237].

[20] BaBar collaboration, J. P. Lees et al., *Evidence for an excess of $\bar{B} \to D^{(*)}\tau^-\bar{\nu}_\tau$ decays*, *Phys. Rev. Lett.* **109** (2012) 101802, [1205.5442].

[21] BaBar collaboration, J. P. Lees et al., *Measurement of an Excess of $\bar{B} \to D^{(*)}\tau^-\bar{\nu}_\tau$ Decays and Implications for Charged Higgs Bosons*, *Phys. Rev.* **D88** (2013) 072012, [1303.0571].

[22] HPQCD collaboration, H. Na, C. M. Bouchard, G. P. Lepage, C. Monahan and J. Shigemitsu, *$B \to Dl\nu$ form factors at nonzero recoil and extraction of $|V_{cb}|$*, *Phys. Rev.* **D92** (2015) 054510, [1505.03925].

[23] D. Bigi and P. Gambino, *Revisiting $B \to D\ell\nu$*, 1606.08030.

[24] S. Fajfer, J. F. Kamenik and I. Nisandzic, *On the $B \to D^*\tau\bar{\nu}_\tau$ Sensitivity to New Physics*, *Phys. Rev.* **D85** (2012) 094025, [1203.2654].

[25] Belle collaboration, A. Abdesselam et al., *Measurement of the branching ratio of $\bar{B}^0 \to D^{*+}\tau^-\bar{\nu}_\tau$ relative to $\bar{B}^0 \to D^{*+}\ell^-\bar{\nu}_\ell$ decays with a semileptonic tagging method*, 1603.06711.

[26] LHCb collaboration, R. Aaij et al., *Measurement of the ratio of branching fractions $\mathcal{B}(\bar{B}^0 \to D^{*+}\tau^-\bar{\nu}_\tau)/\mathcal{B}(\bar{B}^0 \to D^{*+}\mu^-\bar{\nu}_\mu)$*, *Phys. Rev. Lett.* **115** (2015) 111803, [1506.08614].

[27] A. Abdesselam et al., *Measurement of the τ lepton polarization in the decay $\bar{B} \to D^*\tau^-\bar{\nu}_\tau$*, 1608.06391.

[28] M. Tanaka and R. Watanabe, *Tau longitudinal polarization in $B \to D\tau\nu$ and its role in the search for charged Higgs boson*, *Phys. Rev.* **D82** (2010) 034027, [1005.4306].

[29] M. Tanaka and R. Watanabe, *New physics in the weak interaction of $\bar{B} \to D^{(*)}\tau\bar{\nu}$*, *Phys. Rev.* **D87** (2013) 034028, [1212.1878].

[30] U. Nierste, S. Trine and S. Westhoff, *Charged-Higgs effects in a new $B \to D\tau\nu$ differential decay distribution*, *Phys. Rev.* **D78** (2008) 015006, [0801.4938].

[31] A. Datta, M. Duraisamy and D. Ghosh, *Diagnosing New Physics in $b \to c\,\tau\,\nu_\tau$ decays in the light of the recent BaBar result*, *Phys. Rev.* **D86** (2012) 034027, [1206.3760].

[32] Y. Sakaki and H. Tanaka, *Constraints on the charged scalar effects using the forward-backward asymmetry on $B \to D^*\tau\nu$*, *Phys. Rev.* **D87** (2013) 054002, [1205.4908].

[33] A. Crivellin, C. Greub and A. Kokulu, *Explaining $B \to D\tau\nu$, $B \to D^*\tau\nu$ and $B \to \tau\nu$ in a 2HDM of type III*, *Phys. Rev.* **D86** (2012) 054014, [1206.2634].

[34] D. Choudhury, D. K. Ghosh and A. Kundu, *B decay anomalies in an effective theory*, *Phys. Rev.* **D86** (2012) 114037, [1210.5076].

[35] A. Celis, M. Jung, X.-Q. Li and A. Pich, *Sensitivity to charged scalars in $B \to D^{(*)}\tau\nu_\tau$ and $B \to \tau\nu_\tau$ decays*, *JHEP* **01** (2013) 054, [1210.8443].

[36] Y. Sakaki, M. Tanaka, A. Tayduganov and R. Watanabe, *Testing leptoquark models in $\bar{B} \to D^{(*)}\tau\bar{\nu}$*, *Phys. Rev.* **D88** (2013) 094012, [1309.0301].

[37] I. Dorsner, S. Fajfer, N. Kosnik and I. Nisandzic, *Minimally flavored colored scalar in $\bar{B} \to D^{(*)}\tau\bar{\nu}$ and the mass matrices constraints*, *JHEP* **11** (2013) 084, [1306.6493].

[38] M. Duraisamy and A. Datta, *The Full $B \to D^*\tau^-\bar{\nu}_\tau$ Angular Distribution and CP violating Triple Products*, *JHEP* **09** (2013) 059, [1302.7031].

[39] P. Biancofiore, P. Colangelo and F. De Fazio, *On the anomalous enhancement observed in $B \to D^{(*)}\tau\bar{\nu}_\tau$ decays*, *Phys. Rev.* **D87** (2013) 074010, [1302.1042].

[40] M. Duraisamy, P. Sharma and A. Datta, *Azimuthal $B \to D^*\tau^-\bar{\nu}_\tau$ angular distribution with tensor operators*, *Phys. Rev.* **D90** (2014) 074013, [1405.3719].

[41] M. Freytsis, Z. Ligeti and J. T. Ruderman, *Flavor models for $\bar{B} \to D^{(*)}\tau\bar{\nu}$*, *Phys. Rev.* **D92** (2015) 054018, [1506.08896].

[42] A. Greljo, G. Isidori and D. Marzocca, *On the breaking of Lepton Flavor Universality in B decays*, *JHEP* **07** (2015) 142, [1506.01705].

[43] L. Calibbi, A. Crivellin and T. Ota, *Effective field theory approach to $b \to s\ell\ell^{(\prime)}$, $B \to K^{(*)}\nu\bar{\nu}$ and $B \to D^{(*)}\tau\nu$ with third generation couplings*, *Phys. Rev. Lett.* **115** (2015) 181801, [1506.02661].

[44] S. Bhattacharya, S. Nandi and S. K. Patra, *Optimal-observable analysis of possible new physics in $B \to D^{(*)}\tau\nu_\tau$*, *Phys. Rev.* **D93** (2016) 034011, [1509.07259].

[45] C. Hati, G. Kumar and N. Mahajan, *$\bar{B} \to D^{(*)}\tau\bar{\nu}$ excesses in ALRSM constrained from B, D decays and $D^0 - \bar{D}^0$ mixing*, *JHEP* **01** (2016) 117, [1511.03290].

[46] M. Bauer and M. Neubert, *Minimal Leptoquark Explanation for the $R_{D^{(*)}}$, R_K , and $(g-2)_g$ Anomalies*, *Phys. Rev. Lett.* **116** (2016) 141802, [1511.01900].

[47] R. Barbieri, G. Isidori, A. Pattori and F. Senia, *Anomalies in B-decays and $U(2)$ flavour symmetry*, *Eur. Phys. J.* **C76** (2016) 67, [1512.01560].

[48] M. A. Ivanov, J. G. Korner and C. T. Tran, *Exclusive decays $B \to \ell^-\bar{\nu}$ and $B \to D^{(*)}\ell^-\bar{\nu}$ in the covariant quark model*, *Phys. Rev.* **D92** (2015) 114022, [1508.02678].

[49] J. M. Cline, *Scalar doublet models confront ? and b anomalies*, *Phys. Rev.* **D93** (2016) 075017, [1512.02210].

[50] D. Das, C. Hati, G. Kumar and N. Mahajan, *Towards a unified explanation of $R_{D^{(*)}}$, R_K and $(g-2)_\mu$ anomalies in a left-right model with leptoquarks*, *Phys. Rev.* **D94** (2016) 055034, [1605.06313].

[51] M. Bordone, G. Isidori and D. van Dyk, *Impact of leptonic τ decays on the distribution of $B \to P\mu\bar{\nu}$ decays*, *Eur. Phys. J.* **C76** (2016) 360, [1602.06143].

[52] R. Alonso, A. Kobach and J. Martin Camalich, *New physics in the kinematic distributions of $\bar{B} \to D^{(*)}\tau^-(\to \ell^-\bar{\nu}_\ell\nu_\tau)\bar{\nu}_\tau$*, 1602.07671.

[53] S. Nandi, S. K. Patra and A. Soni, *Correlating new physics signals in $B \to D^{(*)}\tau\nu_\tau$ with $B \to \tau\nu_\tau$*, 1605.07191.

[54] F. Feruglio, P. Paradisi and A. Pattori, *Revisiting Lepton Flavour Universality in B Decays*, 1606.00524.

[55] A. K. Alok, D. Kumar, S. Kumbhakar and S. U. Sankar, *D^* polarization as a probe to discriminate new physics in $B \to D^*\tau\bar{\nu}$*, 1606.03164.

[56] S. M. Boucenna, A. Celis, J. Fuentes-Martin, A. Vicente and J. Virto, *Non-abelian gauge extensions for B-decay anomalies*, *Phys. Lett.* **B760** (2016) 214–219, [1604.03088].

[57] S. M. Boucenna, A. Celis, J. Fuentes-Martin, A. Vicente and J. Virto, *Phenomenology of an $SU(2) \times SU(2) \times U(1)$ model with lepton-flavour non-universality*, 1608.01349.

[58] S. Sahoo, R. Mohanta and A. K. Giri, *Explaining R_K and $R_{D^{(*)}}$ anomalies with vector leptoquark*, 1609.04367.

[59] D. A. Faroughy, A. Greljo and J. F. Kamenik, *Confronting lepton flavor universality violation in B decays with high-p_T tau lepton searches at LHC*, 1609.07138.

[60] Z. Ligeti, M. Papucci and D. J. Robinson, *New Physics in the Visible Final States of $B \to D^{(*)}\tau\nu$*, 1610.02045.

[61] M. A. Ivanov, J. G. Korner and C.-T. Tran, *Analyzing new physics in the decays $\bar{B}^0 \to D^{(*)}\tau^-\bar{\nu}_\tau$ with form factors obtained from the covariant quark model*, 1607.02932.

[62] I. Dorsner, S. Fajfer, A. Greljo, J. F. Kamenik and N. Kosnik, *Physics of leptoquarks in precision experiments and at particle colliders*, *Phys. Rept.* **641** (2016) 1–68, [1603.04993].

[63] D. Becirevic, S. Fajfer, N. Kosnik and O. Sumensari, *Leptoquark model to explain the B-physics anomalies, R_K and R_D*, 1608.08501.

[64] B. Grzadkowski, M. Iskrzynski, M. Misiak and J. Rosiek, *Dimension-Six Terms in the Standard Model Lagrangian*, *JHEP* **10** (2010) 085, [1008.4884].

[65] D. Melikhov and B. Stech, *Weak form-factors for heavy meson decays: An Update*, *Phys. Rev.* **D62** (2000) 014006, [hep-ph/0001113].

[66] I. Caprini, L. Lellouch and M. Neubert, *Dispersive bounds on the shape of $\bar{B} \to D^* \ell \bar{\nu}$ form-factors*, *Nucl. Phys.* **B530** (1998) 153–181, [hep-ph/9712417].

[67] Fermilab Lattice, MILC collaboration, J. A. Bailey et al., *Update of $|V_{cb}|$ from the $\bar{B} \to D^* \ell \bar{\nu}$ form factor at zero recoil with three-flavor lattice QCD*, *Phys. Rev.* **D89** (2014) 114504, [1403.0635].

[68] B. Golob. http://indico.ijs.si/getFile.py/access?contribId=1&resId=0&materialId=slides&confId=801, Talk given at "Flavour Physics with High-Luminosity Experiments" in Munich.